J. Appl. Comput. Mech., 9(1) (2023) 274-293
DOI: 10.22055/jacm.2022.40984.3688

ISSN: 2383-4536
jacm.scu.ac.ir

Shahid Chamran University of Ahvaz

Journal of Applied and Computational Mechanics

Research Paper

Analytical Investigations for the Joint Impacts of Electro-osmotic and Some Relevant Parameters to Blood Flow in Mildly Stenosis Artery

Takia Ahmed J. Al-Griffi[1], Abdul-Sattar J. Al-Saif[2]

[1] Department of Mathematics, College of Education for Pure Science, Basrah University, Basrah, Basrah, 61001, Iraq, Email: takiaahmed44@yahoo.com

[2] Department of Mathematics, College of Education for Pure Science, Basrah University, Basrah, Basrah, 61001, Iraq, Email: sattaralsaif@yahoo.com

Received May 31 2022; Revised September 11 2022; Accepted for publication September 11 2022.
Corresponding author: T.A.J. Al-Griffi (takiaahmed44@yahoo.com)

Abstract. The joint impacts of electro-osmotic, variable viscosity, magnetic field, chemical reaction, and porosity on blood flow in the artery slant from the axis at an angle with mild stenosis are investigated using Yang transform homotopy perturbation method (YTHPM). The mathematical model, solved by Tripathi and Sharma, is developed by adding the effect of electro-osmosis. The results of axial velocity, concentration, temperature, and the wall shear stress for blood flow are studied in two cases, the absence and presence of electro-osmosis. The results illustrate that an increase in the electro-osmotic parameter and Helmholtz Smoluchowski velocity leads to velocity increases, while the temperature increases when the Joule heating increases with constant values of electro-osmotic parameter and Helmholtz Smoluchowski velocity. On the contrary, it is noted that the electro-osmotic on concentration has no significant effect. Moreover, the importance of applying electro-osmotic is exhibited through proper use and explaining that how it can benefit physicians during surgical operations. Furthermore, a contour plot is created to show the difference in the profile of velocity to the flow of blood when the magnetic field is increased and the altitude of stenosis takes the larger values. The results exhibit that YTHPM is effective in finding the analytical approximate solutions for Newtonian blood flow under the electro-osmotic parameter influence, with good convergence. In addition, the new solutions' graphs demonstrate the truthfulness, utility, and exigency of YTHPM which are in excellent agreement with the results of earlier investigations.

Keywords: Yang transform homotopy perturbation method (YTHPM), blood flow, mild stenosis arteries, electro-osmotic, variable viscosity, magnetic field and chemical reaction.

1. Introduction

The study of blood flow and its diseases has recently received great interest from scientists and researchers. This interest is due to the fact that the blood transports all the important substances, nutrients and oxygen to all parts of the human body trans arterioles and veins, and this in turn helps to regulate the human body temperature. Because the arteries play a great role in this transfer process, so the study of diseases that affect the arteries has received a great interest in recent times. One of the important diseases that infects the arteries and affects the process of blood flow is atherosclerosis, known as stenosis. This stenosis takes place when fatty substances are deposited on the inner wall of the arteries, which leads to a significant decrease in blood flow to the corresponding body organs, which results in disturbances in the blood circulation. Many scientists and researchers are looking to find solutions for studying the problems of blood flow in arteries that contain stenosis (one or multiple stenosis) by using different methods for different models of blood such as; Ali et al. [1] used finite difference method to study unsteady pulsatile blood flow through a tapered stenosis artery. Mandal et al. [2] applied a finite difference scheme to estimate the effect of externally body acceleration on the laminar pulsatile blood flow through an artery that has a stenosis. Chakravarty and Mandal [3] theoretically solved the nonlinear behavior of blood flow during a single cardiac cycle through an arterial segment with intervening stenosis when subjected to whole-body acceleration. Srivastava et al. [4] investigated the blood flow problem through constriction of the intervening arteries. Zaman et al. [5] analyzed the unstable pulsatile flow of blood through a tapered artery with stenosis. The Carreau model was used to capture the rheology of the blood flowing. At the same time, the study of arteries with stenosis that slants at an angle from the axis, also the impact of magnetic field on blood flow are currently receiving much attention; some of these studies are; Ikbal et al. [6] used finite difference scheme to solve the non-Newtonian blood flow through artery has stenosis in the presence of a transverse magnetic field. Varshney et al. [7] studied numerically the incompressible, non-Newtonian, fully developed, and laminar blood flow in an artery with multiple stenosis under the action of transverse magnetic field. Siddiqui and Geeta [8] utilized a perturbation scheme to study the characteristics of blood flow in slant

Published online: September 22 2022

artery having radially non-symmetrical stenosis. Chitra and Karthikeyan [9] studied analytically the impacts of slip velocity on the unsteady MHD blood flow in an Oscillatory slant tapered artery that has mild stenosis through porous medium. Further, to analyze the effect of the various physical factors of blood flow, the porosity of the midst is a main characteristic of the arteries. On the other hand, the blood viscosity is not constant in a true physiological system, rather it is variable and changes either with the hematocrit percentage or it depends on the pressure and temperature for the artery. Which are (porosity of midst and variable viscosity) also one of the matters received the attention of researchers like; Akram et al. [10] who used the Adomian decomposition method to debate the peristaltic flow of the MHD Newtonian fluid through the hiatus between two coaxial tubes, in which the viscosity of the fluid is treated as variable. Abo-Elkhair et al. [11] studied the effects of external electric field and thickness of the electric double layer on peristaltic pumping of a fluid of variable viscosity through a micro-channel. Coccarelli et al. [12] used a novel method to describe the final boundary conditions in one-dimensional arterial flow networks. The performance of the model based on porous media was examined by several different numerical examples. Govindaraju et al. [13] examined the impact of a porous media of the stenosis arterial wall. The Blood was treated as a non-Newtonian fluid. Several scientists and researchers have recently brought their interest in studying the chemical reaction because of its importance for quantitative prediction of the rate of blood flow and thus helps in diagnosing circulatory diseases and measuring the percentage of glucose in the blood for example; Akbar and Nadeem [14] investigated the impacts of chemical reactions and heat on blood flow in tapered artery that has a stenosis. The model includes a Sisko fluid exemplification of blood flow through axially non-symmetric but radially symmetric stenosis. Mekheimer et al. [15] examined the effect of heat and chemical interactions on blood flow through an anisotropic tapering flexible artery with intervening stenosis. Mwapinga et al. [16] utilized explicit finite difference method to estimate the formulated mathematical model used and developed to study mass transfer and pulsatile blood flow in an artery has a stenosis in the presence of magnetic fields and body accelerations. Misra and Adhikary [17] studied oscillatory MHD blood flow in the presence of an external magnetic field and chemical reaction in a porous arteriole.

Nowadays, the field of electro-kinetics has progressed to become a leading offshoot of fluid mechanics. Reuss in 1809 explained the phenomenon of electro-kinetics which is known by electro-osmotic flow (EOF), which examines fluid flow under the impact of an electric field externally applied. Electro-osmosis in fluid dynamics has many applications and it is applicable to medicines, problems of blood flow and the treating of illness such as cell anomalies and many others. The electrical double layer (EDL) is a fluffy stratum with a lopsided charge. It is formed when a solid surface charged with water or any watery solution is connected. Negative shipments will be formed on this surface, after which the positive ions in the liquid are attracted to this surface and the negative ions alienate, so these unbalanced charges will be formed. If there is an electric field parallel to the solid surface, EDL will positively charge it to move towards the electric field. Many researchers and scientists have recently been interested in this field to study different types of fluids flow [18-23].

Moreover, in 2017, Tripathi and Sharma [24] studied the magnetic field influence on blood flow over a stenosis slant pored artery with heat source and pored media. They suppose that the viscosity of blood flow is variable with variable hematocrit all through the area of the artery. Also, Tripathi and Sharma [25] in 2018, examined the impact of heat transfer on MHD blood flow over a stenosis slant pored artery with heat source by using a homotopy perturbation method. They postulated that the viscosity of blood flow is varying radially with hematocrit all through the area of the artery. In the same year, Tripathi and Sharma [26] utilized the shooting method to illustrate the impact of viscous squandering and Joule heating on unstable two-phase blood flow during a stenosis artery in the existence of a changing magnetic field. They consider the viscosity a constant for cell-free plasma stratum whilst it's a function of the hematocrit level for the core. Moreover; in 2018 Tripathi and Sharma [27] examined the impacts of mass and heat transfer on blood flow arterial under a chemical reaction effect with a magnetic field applied. They hypothesized that in a non-tapered artery slanting at angles the stenosis is mild and the viscosity is variable and varying with the hematocrit ratio. Abubakar and Adeoye [28] in 2019, used the differential transform method (DTM) to analyze the effect of the magnetic field with radiation for the pored tapered slant stenosis artery. Also, they assumed that the viscosity is variable. Saleem et al. [29] in 2020, discuss the blood flow through a catheterized artery that has a mild stenosis in the wall with a blood clot in the center. They used the Newtonian viscous fluid model and also distinct forms of stenosis (that is, symmetric and non-symmetric shapes) for this study. In 2021, Hasen and Abdulhadi [30] investigated the joint electro-osmotic peristaltic transport with mass and transferring heat with the existence of the Joule electro-thermal heating through a micro-channel filled by Rabinowitsch fluid. They take the viscosity as constant. Akhtar et al. [31] in 2021, evaluated mathematically the electro-osmotically modulated hemodynamic through the artery that have multiple stenoses. The non-Newtonian behavior of blood flow is addressed through the use of the Casson fluid model of this flow problem. Saleem et al. [32] in 2021, studied the peristaltic flow of Bingham visco-plastic micro-polar fluid flow inside a micro-length channel with electro-osmotic impacts. The electro-osmotic impacts are generated due to an axially applied electric field. Shahzad et al. [33] in 2022, studied the electro-osmotic effects of a blood-based hybrid Nano-fluid flow through an artery with multiple stenoses. The achieved solutions are graphically analyzed for both symmetric and non-symmetric forms of stenosis. For different values of flow rate and electro-osmotic parameter, the streamlines are analyzed. Saleem et al. [34] in 2022, illustrated the electro-osmotically modulated hemodynamic within a stenosis artery, considering cases of symmetric and non-symmetric stenosis for the first time. The blood is treated as an aqueous ion solution.

Despite the above mentioned studies, the combined influence of electro-osmosis, Joule heating, variable viscosity, magnetic field, chemical reaction, mass and heat transfer on blood flow has not been taken into consideration (to our knowledge). Therefore, the aims of this study are: firstly, studying the joint impacts of electro-osmotic, Joule heating, variable viscosity, magnetic field, chemical reaction, mass and heat transfer on blood flow. Secondly, we develop a model in Ref. [27] by adding electro-osmosis effect and Joule heating on it. According to our humble information, the new system has not been studied before; this will be one of the new points of innovation in our work. Third, we solve the new system by applying the new method (YTHPM) which was proposed for first time in [35, 36]. Fourth, we studied the impacts of electro-osmotic parameter, Joule heating, Helmholtz Smoluchowski velocity, penchant angle, magnetic field, porosity parameter and chemical reaction of axial velocity, concentration, temperature and the wall shear stress. Finally, we analyzed the convergence of the results with and without the existence of the electro-osmotic. Moreover, the advantage of the new method is that all the results are obtained through the 1st iteration. The numerical results, obtained by using YTHPM for solving the current problem under study; confirming the effectiveness, competence, and high accuracy of this method and also its results agree well with those reported by other researchers in the field.

In addition, the novelty of the current paper lies in the development of the mathematical model solved by the researchers in Ref. [27] by adding the effect of electro-osmosis. Moreover, we have solved the current problem by using a developed and novel method that has not been used before in two cases, the presence and absence of the effect of electro-osmosis. This method gives new and high-accuracy results which confirms its validity by comparison with previous studies in the literature. Moreover, the new study (i.e. adding effect of electro-osmosis) with the applications of (variable viscosity, magnetic field, chemical reaction and porosity) explains the importance of applying electro-osmosis and how doctors can benefit from it during surgeries through proper use.

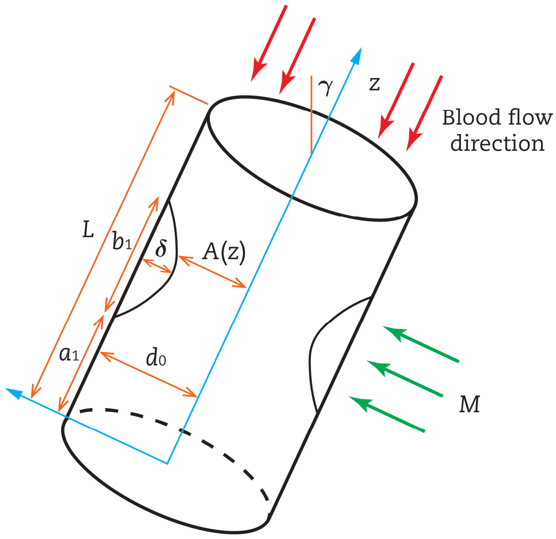

Fig. 1. The slant artery's geometry with a magnetic field applied columnar.

2. The Mathematical Formulation

Meditation of the blood flow in two-dimensional through a pored artery has stenosis with length L, slant by an angle γ from the cephalic axis. Suppose the flow of fluid is incompressible, Newtonian, axially symmetric and bio-magnetic. A regular magnetic field was applied only columnar to the orientation for the slant artery [27], as shown in Fig. 1.

Suppose the variable viscosity changing with variable hematocrit of density ρ in a radial trend, the artery shape is cylindrical. By these suppositions, the governing equations (continuity, momentum, heat and mass concentration) under the influence of electro-osmotic and Joule heating together with the impacts of variable viscosity, magnetic field, chemical reaction may be written as follows:

$$\frac{\partial \hat{u}}{\partial \hat{r}}+\frac{\hat{u}}{\hat{r}}+\frac{\partial \hat{w}}{\partial \hat{z}}=0 \tag{1}$$

$$\rho\left(\hat{u}\frac{\partial \hat{u}}{\partial \hat{r}}+\hat{w}\frac{\partial \hat{u}}{\partial \hat{z}}\right)=-\frac{\partial \hat{P}}{\partial \hat{r}}+\frac{\partial}{\partial \hat{r}}\left[2\mu(\hat{r})\frac{\partial \hat{u}}{\partial \hat{r}}\right]+\frac{2\mu(\hat{r})}{\hat{r}}\left[\frac{\partial \hat{u}}{\partial \hat{r}}-\frac{\hat{u}}{\hat{r}}\right]+\frac{\partial}{\partial \hat{z}}\left[\mu(\hat{r})\left(\frac{\partial \hat{u}}{\partial \hat{z}}+\frac{\partial \hat{w}}{\partial \hat{r}}\right)\right] \tag{2}$$

$$\begin{aligned}\rho\left(\hat{u}\frac{\partial \hat{w}}{\partial \hat{r}}+\hat{w}\frac{\partial \hat{w}}{\partial \hat{z}}\right)=&-\frac{\partial \hat{P}}{\partial \hat{z}}+\frac{\partial}{\partial \hat{z}}\left[2\mu(\hat{r})\frac{\partial \hat{w}}{\partial \hat{z}}\right]+\frac{1}{\hat{r}}\frac{\partial}{\partial \hat{r}}\left[\hat{r}\mu(\hat{r})\left(\frac{\partial \hat{u}}{\partial \hat{z}}+\frac{\partial \hat{w}}{\partial \hat{r}}\right)\right]-\sigma^{*}\hat{\mu}_{m1}^{2}H_0^2\,\hat{w}\\&+\rho\alpha g\left(\hat{T}-\hat{T}_0\right)\cos(\gamma)+\rho\alpha g\left(\hat{C}-\hat{C}_0\right)\cos(\gamma)-\frac{\mu(\hat{r})}{\kappa^{*}}\hat{w}+\rho_e^{\bullet}E^{\bullet}\end{aligned} \tag{3}$$

$$\rho c_p\left(\hat{u}\frac{\partial \hat{T}}{\partial \hat{r}}+\hat{w}\frac{\partial \hat{T}}{\partial \hat{z}}\right)=\frac{k_1^{\bullet}}{\hat{r}}\frac{\partial}{\partial \hat{r}}\left(\hat{r}\frac{\partial \hat{T}}{\partial \hat{r}}\right)+\mu(\hat{r})\left(\frac{\partial \hat{w}}{\partial \hat{r}}\right)^2+S \tag{4}$$

$$\left(\hat{u}\frac{\partial \hat{C}}{\partial \hat{r}}+\hat{w}\frac{\partial \hat{C}}{\partial \hat{z}}\right)=D\left(\frac{\partial^2 \hat{C}}{\partial \hat{r}^2}+\frac{1}{\hat{r}}\frac{\partial \hat{C}}{\partial \hat{r}}+\frac{\partial^2 \hat{C}}{\partial \hat{z}^2}\right)+\frac{DK_T}{T_m}\left(\frac{\partial^2 \hat{T}}{\partial \hat{r}^2}+\frac{1}{\hat{r}}\frac{\partial \hat{T}}{\partial \hat{r}}+\frac{\partial^2 \hat{T}}{\partial \hat{z}^2}\right)-L\left(\hat{C}-\hat{C}_0\right) \tag{5}$$

The boundary conditions are:

$$\frac{\partial \hat{w}}{\partial \hat{r}}=0,\ \frac{\partial \hat{C}}{\partial \hat{r}}=0,\ \frac{\partial \hat{T}}{\partial \hat{r}}=0 \quad \text{at} \quad \hat{r}=0 \quad (\text{ i.e. along central (symmetric) axis of the tube}) \tag{6a}$$

$$\hat{w}=0,\hat{C}=0,\ \hat{T}=0 \quad \text{at} \quad \hat{r}=\hat{A}(\hat{z}) \quad (\text{i.e. at the wall of artery}) \tag{6b}$$

where, $\hat{A}(\hat{z})$ is the geometry function defined as [27]:

$$\hat{A}(\hat{z})=\begin{cases}\left(1-\eta^{\bullet}\left[b_1^{n-1}\left(\hat{z}-a_1\right)-\left(\hat{z}-a_1\right)^n\right]\right)\hat{d}_1(\hat{z}), & a_1\le\hat{z}\le a_1+b_1,\\ \hat{d}_1(\hat{z}), & \text{otherwise.}\end{cases} \tag{6c}$$

where, $\hat{d}_1(\hat{z})=d_0+\xi^{\bullet}\hat{z};\ \xi^{\bullet}=\tan(\phi);\ \eta^{\bullet}=(\delta^{\bullet}n^{n/(n-1)})/[(d_0b_1^n)(n-1)]$, $\delta^{\bullet}$ is the stenosis height fall in $\hat{z}=a_1+b_1/n^{n/(n-1)}$; b_1 is the stenosis length and a_1 is the distance between the entrance and beginning of the stenosis. While n is the parameter that defines the form for the stenosis, when n = 2 gives the stenosis have the symmetrical form and if $n\ge 2$ the stenosis is non-symmetric.

The variable viscosity for the blood flow is defined by [27]:

$$\mu(\hat{r}) = \mu_0\left(1 + \lambda^* h^*(\hat{r})\right) \tag{7a}$$

where,

$$h^*(\hat{r}) = H\left(1 - \left[\frac{\hat{r}}{d_0}\right]^m\right) \tag{7b}$$

Let $\lambda^* H = H_r, \lambda^*$ is constant that takes the value 2.5, and *m* determines the exact form of the velocity. The Joule heating defines as [18]:

$$S = i_e^2\sigma;\;\; i_e^2 = \frac{E^\bullet}{\sigma} \tag{8a}$$

Depended on Poisson-Boltzmann equation, then we have:

$$\nabla^2\hat{\Phi} = -\frac{\rho_e^\bullet}{\ell^*} \tag{8b}$$

where, $\rho_e^\bullet = e z^\bullet(n^+ - n^-)$. From Boltzmann distribution, the values of ions can be determined in the case when EDL does not exist as follows:

$$n^{\pm} = n_0^* \exp\left(\mp\frac{z^\bullet e\ddot{\Phi}}{k_B^* T_{av}^*}\right) \tag{9}$$

where, k_B^*, n_0^*, T_{av}^* are the constant of Boltzmann, bulk size concentration of negative or positive ions, and the local absolute temperature of the electrolytic solution. Therefore:

$$\rho_e^\bullet = -2z^\bullet e n_0^* \sinh\left(\frac{z^\bullet e\ddot{\Phi}}{k_B^* T_{av}^*}\right) \tag{10}$$

By putting (9) into (8), we get:

$$\nabla^2\hat{\Phi} = \frac{2z^\bullet e n_0^* \sinh\left(\frac{z^\bullet e\hat{\Phi}}{k_B^* T_{av}^*}\right)}{\ell^*} \tag{11}$$

From Debye Huckel supposition, $\sinh(z^\bullet e\hat{\Phi} / k_B^* T_{av}^*) \approx z^\bullet e\hat{\Phi} / k_B^* T_{av}^*$. To simplify, let the non-dimensional define as: $\Phi = \hat{\Phi} / \varsigma$ and $r = \hat{r} / d_0$. Then we have:

$$\nabla^2\Phi = m_0^2\Phi \tag{12}$$

with the following boundary conditions: $\partial\Phi / \partial r = 0$ at $r = 0$ and $\Phi = 1$ at $r = A(z)$. Then, the exact solution is:

$$\Phi = \frac{I_0(r m_0)}{I_0(m_0 A(z))} \tag{13}$$

3. The Dimensionless Set [18, 27]

Consider the non-dimensional set defined as follows:

$$\hat{r} = r d_0,\, \hat{z} = z b_1,\, \hat{A} = A d_0,\, \hat{u} = \frac{u u_0 \delta}{b_1},\, \hat{w} = w u_0,\, \hat{P} = \frac{u_0 b_1 \mu_0}{d_0^2}P,\, T = \frac{\hat{T} - \hat{T}_0}{\hat{T}_0},\, C = \frac{\hat{C} - \hat{C}_0}{\hat{C}_0},\, \mathrm{Re} = \frac{\rho u_0 b_1}{\mu_0},\, E_c = \frac{u_0^2}{c_p \hat{T}_0},\, \mathrm{Pr} = \frac{c_p \mu}{k_1^\bullet},$$

$$S_r = \frac{\rho D K_T \hat{T}_0}{\mu_0 \hat{C}_0 T_m},\, S_c = \frac{\mu_0}{D\rho},\, Z = \frac{\kappa^*}{d_0^2},\, M^2 = \frac{\sigma H_0^2 d_0^2}{\mu_0},\, E = \frac{\rho d_0^2 L}{\mu},\, U_{hs} = \frac{E^\bullet \ell^* \varsigma}{\mu u_0},\, S = \frac{E^{\bullet 2} d_0^2}{\sigma\left(\hat{T}_0 - \hat{T}_1\right)\kappa^*},\, m_0 = d_0 e z^\bullet\sqrt{\frac{2n_0}{\ell^* K_B^* T_{av}}} = \frac{d_0}{\lambda_d^*}$$

The non-dimensional viscosity is:

$$\mu(r) = \mu_0\left(1 + \lambda^* H(1 - r^m)\right) \tag{14}$$

The non-dimensional geometry defined as when $d_0 = 1$,

$$A(z) = \begin{cases} \left(1 - \eta_1^\bullet\left[(z - \ell_1) - (z - \ell_1)^n\right]\right)\left(1 + \xi_1^\bullet z\right), & \ell_1 \le z \le \ell_1 + 1, \\ 1, & \text{otherwise.} \end{cases} \tag{15}$$

where, $\xi_1^\bullet = \xi^\bullet b_1 / d_0$, $\eta_1^\bullet = \delta n^{\frac{n}{n-1}} / (n-1), \delta = \delta^\bullet / d_0$ and $\ell_1 = a_1 / b_1$.

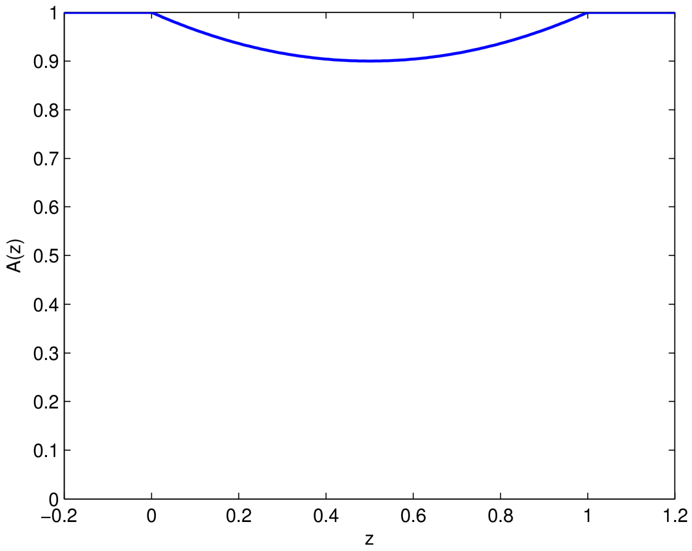

Fig. 2. The geometry function form for the slant artery's in the considered system.

The schematic configuration of the considered system for Fig. 1 can be seen in Fig. 2. Therefore, the governing equations (1)-(5) in non-dimensional forms are as follows:

$$\frac{\partial w}{\partial z}=0 \tag{16}$$

$$\frac{\partial P}{\partial r}=0 \tag{17}$$

$$\frac{\partial P}{\partial z}=\left[\frac{1}{r}+H_r\left(\frac{1}{r}-(m+1)\,r^{m-1}\right)\right]\frac{\partial w}{\partial r}+\left[1+H_r\left(1-r^m\right)\frac{\partial}{\partial r}\left(\frac{\partial w}{\partial r}\right)\right]+G_r\,T\cos(\gamma)+G_m\,C\cos(\gamma)-w\left(M^2+\frac{1}{Z}+\frac{H_r}{Z}\left(1-r^m\right)\right)+U_{hs}\,m_0^2\,\frac{I_0(m_0\,r)}{I_0(m_0\,A)} \tag{18}$$

$$\frac{1}{r}\frac{\partial}{\partial r}\left(r\frac{\partial T}{\partial r}\right)+E_c\,P_r\left(\frac{\partial w}{\partial r}\right)^2+S=0 \tag{19}$$

$$\frac{1}{S_c}\frac{1}{r}\frac{\partial}{\partial r}\left(r\frac{\partial C}{\partial r}\right)+S_r\left(\frac{1}{r}\frac{\partial}{\partial r}\left(r\frac{\partial T}{\partial r}\right)\right)-EC=0 \tag{20}$$

The initial conditions in electro-osmotic field absence can be defined as follows:

$$w(r,z,0)=\left(\frac{r^2-A(z)^2}{4}\right)\left(M^2+\frac{1}{Z}\right)\frac{\partial P}{\partial z},\qquad T(r,z,0)=\left(\frac{r^2-A(z)^2}{4}\right),\qquad C(r,z,0)=-\left(\frac{r^2-A(z)^2}{4}\right)$$

and the initial conditions when electro-osmotic field presence is defined as:

$$w(r,z,0)=\left(\frac{r^2-A(z)^2}{4}\right)\left(M^2+\frac{1}{Z}\right)\frac{\partial P}{\partial z}-U_{hs}\left(\left[\frac{I_0\left(\sqrt{m_0 r}\right)}{I_0\left(\sqrt{m_0 A(z)}\right)}\right]-1\right),$$

$$T(r,z,0)=\left(\frac{r^2-A(z)^2}{4}\right)-S\left(\left[\frac{I_0\left(\sqrt{m_0 r}\right)}{I_0\left(\sqrt{m_0 A(z)}\right)}\right]-1\right),$$

$$C(r,z,0)=-\left(\frac{r^2-A(z)^2}{4}\right)$$

The boundary conditions are:

$$\frac{\partial w}{\partial r}(r,z,t)=0,\quad \frac{\partial C}{\partial r}(r,z,t)=0,\quad \frac{\partial T}{\partial r}(r,z,t)=0\quad \text{at}\quad r=0 \tag{21a}$$

$$w(r,z,t)=0,\quad C(r,z,t)=0,\quad T(r,z,t)=0\quad \text{at}\quad r=A(z) \tag{21b}$$

4. Implementation of YTHPM

In this section, we apply the YTHPM, that is dependent on both algorithms of YT and HPM illustrated in [35, 36], to Equations (18-20), and the following steps are illustrated the fundamental ideas of its application:

Step 1: By using HPM, we get:

$$\frac{\partial w}{\partial r}-w_0^{\bullet}+\beta w_0^{\bullet}+\beta\left(r\frac{\partial P}{\partial z}-rH_r\left(\frac{1}{r}-(m+1)\,r^{m-1}\right)\frac{\partial w}{\partial r}-r\left[1+H_r\left(1-r^m\right)\frac{\partial}{\partial r}\left(\frac{\partial w}{\partial r}\right)\right]-rG_r\,T\cos(\gamma)+rG_m\,C\cos(\gamma)\right)$$
$$+\beta\left(rw\left(M^2+\frac{1}{Z}+\frac{H_r}{Z}\left(1-r^m\right)\right)-rU_{hs}\,m_0^2\frac{I_0(m_0 r)}{I_0(m_0 A)}\right)=0$$

$$\frac{\partial T}{\partial r}-T_0^{\bullet}+\beta T_0^{\bullet}+\beta\left(r\frac{\partial^2 T}{\partial r^2}+rE_c\,P_r\left(\frac{\partial w}{\partial r}\right)^2-rS\right)=0$$

$$\frac{\partial C}{\partial r}-C_0^{\bullet}+\beta C_0^{\bullet}+\beta\left(r\frac{\partial^2 C}{\partial r^2}+rS_c\,S_r\left(\frac{1}{r}\frac{\partial}{\partial r}\left(r\frac{\partial T}{\partial r}\right)\right)-rEC\right)=0$$

Step 2: By taking the Yang transform to the above equations in step (1) for both sides, we obtain:

$$\frac{1}{s}\tilde{w}-w(0)-Y(w_0^{\bullet})+Y(\beta w_0^{\bullet})+Y\left[\beta\left(r\frac{\partial P}{\partial z}-rH_r\left(\frac{1}{r}-(m+1)\,r^{m-1}\right)\frac{\partial w}{\partial r}-r\left[1+H_r\left(1-r^m\right)\frac{\partial}{\partial r}\left(\frac{\partial w}{\partial r}\right)\right]-rG_r\,T\cos(\gamma)\right)\right]$$
$$+Y\left[\beta\left(rw\left(M^2+\frac{1}{Z}+\frac{H_r}{Z}\left(1-r^m\right)\right)-rU_{hs}\,m_0^2\frac{I_0(m_0 r)}{I_0(m_0 A)}-rG_m\,C\cos(\gamma)\right)\right]=0$$

$$\frac{1}{s}\tilde{T}-T(0)-Y(T_0^{\bullet})+Y(\beta T_0^{\bullet})+Y\left[\beta\left(r\frac{\partial^2 T}{\partial r^2}+rE_c\,P_r\left(\frac{\partial w}{\partial r}\right)^2-rS\right)\right]=0$$

$$\frac{1}{s}\tilde{C}-C(0)-Y(C_0^{\bullet})+Y(\beta C_0^{\bullet})+Y\left[\beta\left(r\frac{\partial^2 C}{\partial r^2}+rS_c\,S_r\left(\frac{1}{r}\frac{\partial}{\partial r}\left(r\frac{\partial T}{\partial r}\right)\right)-rEC\right)\right]=0$$

where $w_0^{*}=w(0)=w(r,z,0)$, $T_0^{*}=T(0)=T(r,z,0)$ and $C_0^{*}=C(0)=C(r,z,0)$ are the initial conditions. The rearrangement of the above equations yields:

$$\tilde{w}=s\,w(0)+s\,Y(w_0^{\bullet})-s\,Y(\beta w_0^{\bullet})-s\,Y\left[\beta\left(r\frac{\partial P}{\partial z}-rH_r\left(\frac{1}{r}-(m+1)\,r^{m-1}\right)\frac{\partial w}{\partial r}-r\left[1+H_r\left(1-r^m\right)\frac{\partial}{\partial r}\left(\frac{\partial w}{\partial r}\right)\right]\right)\right]$$
$$-s\,Y\left[\beta\left(rw\left(M^2+\frac{1}{Z}+\frac{H_r}{Z}\left(1-r^m\right)\right)-rU_{hs}\,m_0^2\frac{I_0(m_0 r)}{I_0(m_0 A)}-rG_m\,C\cos(\gamma)-rG_r\,T\cos(\gamma)\right)\right] \tag{22a}$$

$$\tilde{T}=s\,T(0)+s\,Y(T_0^{\bullet})-s\,Y(\beta T_0^{\bullet})-s\,Y\left[\beta\left(r\frac{\partial^2 T}{\partial r^2}+rE_c\,P_r\left(\frac{\partial w}{\partial r}\right)^2-rS\right)\right] \tag{22b}$$

$$\tilde{C}=s\,C(0)+s\,Y(C_0^{\bullet})-s\,Y(\beta C_0^{\bullet})-s\,Y\left[\beta\left(r\frac{\partial^2 C}{\partial r^2}+rS_c\,S_r\left(\frac{1}{r}\frac{\partial}{\partial r}\left(r\frac{\partial T}{\partial r}\right)\right)-rEC\right)\right] \tag{22c}$$

Step 3: Taking YT inverse of both sides of Equations (22a)-(22c), we have:

$$w=Y^{-1}(s\,w(0))+Y^{-1}(s\,Y(w_0^{\bullet}))-Y^{-1}(s\,Y(\beta w_0^{\bullet}))-Y^{-1}\left(s\,Y\left[\beta\left(r\frac{\partial P}{\partial z}-rH_r\left(\frac{1}{r}-(m+1)\,r^{m-1}\right)\frac{\partial w}{\partial r}-r\left[1+H_r\left(1-r^m\right)\frac{\partial}{\partial r}\left(\frac{\partial w}{\partial r}\right)\right]\right)\right]\right)$$
$$-Y^{-1}\left(s\,Y\left[\beta\left(rw\left(M^2+\frac{1}{Z}+\frac{H_r}{Z}\left(1-r^m\right)\right)-rU_{hs}\,m_0^2\frac{I_0(m_0 r)}{I_0(m_0 A)}-rG_m\,C\cos(\gamma)-rG_r\,T\cos(\gamma)\right)\right]\right)$$

$$T=Y^{-1}(s\,T(0))+Y^{-1}(s\,Y(T_0^{\bullet}))-Y^{-1}(s\,Y(\beta T_0^{\bullet}))-Y^{-1}\left(s\,Y\left[\beta\left(r\frac{\partial^2 T}{\partial r^2}+rE_c\,P_r\left(\frac{\partial w}{\partial r}\right)^2-rS\right)\right]\right)$$

$$C=Y^{-1}(sC(0))+Y^{-1}(s\,Y(C_0^{\bullet}))-Y^{-1}(s\,Y(\beta C_0^{\bullet}))-Y^{-1}\left(s\,Y\left[\beta\left(r\frac{\partial^2 C}{\partial r^2}+rS_c\,S_r\left(\frac{1}{r}\frac{\partial}{\partial r}\left(r\frac{\partial T}{\partial r}\right)\right)-rEC\right)\right]\right)$$

Step 4: From the assumption of the HPM that puts $w = w_0 + \beta w_1 + \beta^2 w_2 + \ldots$, $T = T_0 + \beta T_1 + \beta^2 T_2 + \ldots$ and $C = C_0 + \beta C_1 + \beta^2 C_2 + \ldots$, then we have:

$$
\begin{aligned}
w_0 + \beta w_1 + \beta^2 w_2 + \ldots = {} & Y^{-1}(s\,w(0)) + Y^{-1}(s\,Y(w_0^{\bullet})) - Y^{-1}(s\,Y(\beta w_0^{\bullet})) - Y^{-1}\left(s\,Y\left[\beta\left(-r H_r\left(\frac{1}{r} - (m+1)\, r^{m-1}\right)\frac{\partial}{\partial r}(w_0 + \beta w_1 + \beta^2 w_2 + \ldots)\right)\right]\right) \\
& - Y^{-1}\left(s\,Y\left[\beta\left(r\frac{\partial P}{\partial z} - r\left[1 + H_r(1 - r^m)\frac{\partial}{\partial r}\left(\frac{\partial}{\partial r}(w_0 + \beta w_1 + \beta^2 w_2 + \ldots)\right)\right] + r(w_0 + \beta w_1 + \beta^2 w_2 + \ldots)\left(M^2 + \frac{1}{Z} + \frac{H_r}{Z}(1 - r^m)\right)\right)\right]\right) \\
& - Y^{-1}\left(s\,Y\left[\beta\left(-r U_{hs}\, m_0^2 \frac{I_0(m_0 r)}{I_0(m_0 A)} - r G_m (C_0 + \beta C_1 + \beta^2 C_2 + \ldots)\cos(\gamma) - r\, G_r (T_0 + \beta T_1 + \beta^2 T_2 + \ldots)\cos(\gamma)\right)\right]\right)
\end{aligned}
$$

$$
\begin{aligned}
T_0 + \beta T_1 + \beta^2 T_2 + \ldots = {} & Y^{-1}(s\,T(0)) + Y^{-1}(s\,Y(T_0^{\bullet})) - Y^{-1}(s\,Y(\beta T_0^{\bullet})) - Y^{-1}\left(s\,Y\left[\beta\left(r\frac{\partial^2}{\partial r^2}(T_0 + \beta T_1 + \beta^2 T_2 + \ldots)\right)\right]\right) \\
& - Y^{-1}\left(s\,Y\left[\beta\left(r E_c P_r\left(\frac{\partial}{\partial r}(w_0 + \beta w_1 + \beta^2 w_2 + \ldots)\right)^2 - r S\right)\right]\right)
\end{aligned}
$$

$$
\begin{aligned}
C_0 + \beta C_1 + \beta^2 C_2 + \ldots = {} & Y^{-1}(s\,C(0)) + Y^{-1}(s\,Y(C_0^{\bullet})) - Y^{-1}(s\,Y(\beta C_0^{\bullet})) - Y^{-1}\left(s\,Y\left[\beta\left(r\frac{\partial^2}{\partial r^2}(C_0 + \beta C_1 + \beta^2 C_2 + \ldots)\right)\right]\right) \\
& - Y^{-1}\left(s\,Y\left[\beta\left(r S_c S_r\left(\frac{1}{r}\frac{\partial}{\partial r}\left(r\frac{\partial}{\partial r}(T_0 + \beta T_1 + \beta^2 T_2 + \ldots)\right)\right) - r E (C_0 + \beta C_1 + \beta^2 C_2 + \ldots)\right)\right]\right)
\end{aligned}
$$

Step 5: By equating terms that have the same power of β, we get:

$$
\beta^0 : \begin{cases}
w_0 = Y^{-1}(s\,w(0)) + Y^{-1}(s\,Y(w_0^{*})) \\
T_0 = Y^{-1}(s\,T(0)) + Y^{-1}(s\,Y(T_0^{*})) \\
C_0 = Y^{-1}(s\,C(0)) + Y^{-1}(s\,Y(C_0^{*}))
\end{cases}
$$

$$
\beta^1 : \begin{cases}
w_1 = -Y^{-1}(s\,Y(w_0^{*})) - Y^{-1}\left(s\,Y\left[-r H_r\left(\frac{1}{r} - (m+1)\, r^{m-1}\right)\frac{\partial w_0}{\partial r} + r\frac{\partial P}{\partial z} - r\left[1 + H_r(1 - r^m)\frac{\partial}{\partial r}\left(\frac{\partial w_0}{\partial r}\right)\right] - r\, G_r (T_0)\cos(\gamma) + r(w_0)\left(M^2 + \frac{1}{Z} + \frac{H_r}{Z}(1 - r^m)\right)\right.\right. \\
\qquad \left.\left. - r U_{hs}\, m_0^2 \frac{I_0(m_0 r)}{I_0(m_0 A)} - r G_m (C_0)\cos(\gamma)\right]\right) \\
T_1 = -Y^{-1}(s\,Y(T_0^{\bullet})) - Y^{-1}\left(s\,Y\left[r\frac{\partial^2 T_0}{\partial r^2} + r E_c P_r\left(\frac{\partial w_0}{\partial r}\right)^2 - r S\right]\right) \\
C_1 = -Y^{-1}(s\,Y(C_0^{\bullet})) - Y^{-1}\left(s\,Y\left[r\frac{\partial^2 C_0}{\partial r^2} + r S_c S_r\left(\frac{1}{r}\frac{\partial}{\partial r}\left(r\frac{\partial T_0}{\partial r}\right)\right) - r E (C_0)\right]\right) \\
\vdots
\end{cases}
$$

so on.

Step 6: The analytical approximate solutions can be obtained by putting $\beta = 1$,

$$
\begin{aligned}
w &= \lim_{\beta \to 1} w = w_0 + w_1 + w_2 + \cdots \\
T &= \lim_{\beta \to 1} T = T_0 + T_1 + T_2 + \cdots \\
C &= \lim_{\beta \to 1} C = C_0 + C_1 + C_2 + \cdots
\end{aligned}
$$

So, the analytical solutions for Equations (18)-(20), firstly when electro-osmotic field absence are:

$$
\begin{aligned}
w = {} & \left(\frac{r^2 - A(z)^2}{4}\right)\left(M^2 + \frac{1}{Z}\right)\frac{\partial P}{\partial z} + \frac{r^2 \sin\left(\frac{\gamma}{2}\right)^2 (G_m - G_r)\left(3A(z) - r^3 - \frac{r^4}{4}\right)}{12} - \frac{r^2 M^2 H_r \frac{\partial P}{\partial z}(m!\, r^{m+1})}{4} \\
& - \frac{r^2 M^2 \frac{\partial P}{\partial z}\left(3A(z) - r^3 - \frac{r^4}{4}\right)\left(H_r - H_r \frac{m!\, r^{m+1}}{(m+1)!}\right)}{24 Z} - E S_c G_m \cos(\gamma)\frac{r^2}{2}\left(\frac{A(z)^2}{4} - \frac{r^3}{12} - \frac{r^4}{48}\right) + \ldots
\end{aligned}
$$

$$
T = \left(\frac{r^2 - A(z)^2}{4}\right) + \left(\frac{\partial P}{\partial z}\right)^2 E_c P_r\, r\left[\frac{r^2 \sin\left(\frac{\gamma}{2}\right)^2 (G_m - G_r)(r^3 + 3r^2)}{12} - \frac{r^2 M^2 \frac{\partial P}{\partial z}(r^3 + 3r^2)\left(H_r - H_r \frac{m!\, r^{m+1}}{(m+1)!}\right)}{24 Z} + \frac{r M^2 H_r \frac{\partial P}{\partial z}(m!\, r^{m+1})}{2} + \ldots\right]^2
$$

$$C=-\left(\frac{r^2-A(z)^2}{4}\right)+\frac{\partial P}{\partial z}\left(\frac{r^2}{2}\left(\frac{r}{2}+\frac{1}{2}\right)+ES_c\left(\frac{A(z)^2}{4}-\frac{r^3}{12}-\frac{r^4}{48}\right)-\frac{ES_c S_r P_r\left[72G_m A(z)^2\cos(\gamma)-72G_r A(z)^2\cos(\gamma)\right]}{144}\right.$$
$$\left.+\frac{ES_c S_r P_r M^4 H_r{}^2 r^{m+2}\left(\frac{\partial P}{\partial z}\right)^2\left(\frac{r^4}{4}+r^3-3A(z)^2\right)\left[m(m+1)!(m-1)!r^4+24Zr(m!)^2-12m(m+1)!(m-1)!A(z)^2+\ldots\right]}{576\left(m!(m+1)!\right)Z^2}+\ldots\right)$$

Secondly, when the electro-osmotic field presence are:

$$w=\left(\frac{r^2-A(z)^2}{4}\right)\left(M^2+\frac{1}{Z}\right)\frac{\partial P}{\partial z}-U_{hs}\left(\left[\frac{I_0(\sqrt{m_0}\,r)}{I_0(\sqrt{m_0}\,A(z))}\right]-1\right)-H_r\frac{r^2}{2}r^{m-1}(m+1)U_{hs}\left(\left[\frac{I_0(\sqrt{m_0}\,r)}{I_0(\sqrt{m_0}\,A(z))}\right]-1\right)$$
$$-ES_c\frac{r^2}{2}G_m\cos(\gamma)\left(\frac{A(z)^2}{4}-\frac{r^3}{12}-\frac{r^4}{4}\right)+\ldots$$

$$T=\left(\frac{r^2-A(z)^2}{4}\right)-S\left(\left[\frac{I_0(\sqrt{m_0}\,r)}{I_0(\sqrt{m_0}\,A(z))}\right]-1\right)+\left(\frac{\partial P}{\partial z}\right)^2\left[E_cP_r\frac{r^2}{2}\left(\left[M^2+\frac{1}{Z}-\frac{H_r r^m}{Z}\right]\left[U_{hs}\left(\left[\frac{I_0(\sqrt{m_0}\,r)}{I_0(\sqrt{m_0}\,A(z))}\right]-1\right)\right]\right)^2\right]$$
$$+\left(\frac{\partial P}{\partial z}\right)^2E_cP_r\frac{r^2}{2}\left(\cos(\gamma)\left[G_r\left(\frac{A(z)^2}{4}-\frac{r^3}{12}-\frac{r^4}{4}+2S\left(\left[\frac{I_0(\sqrt{m_0}\,r)}{I_0(\sqrt{m_0}\,A(z))}\right]-1\right)\right)-G_m\left(\frac{A(z)^2}{4}-\frac{r^3}{12}-\frac{r^4}{4}\right)\right]\right)^2+\ldots$$

$$C=-\left(\frac{r^2-A(z)^2}{4}\right)+\frac{\partial P}{\partial z}\left(SS_cS_r\,r+E_cS_cS_rP_rM^4r^3\left[U_{hs}\left(\left[\frac{I_0(\sqrt{m_0}\,r)}{I_0(\sqrt{m_0}\,A(z))}\right]-1\right)\right]^2-\frac{ES_cP_r\left[72G_mA(z)^2\cos(\gamma)-72G_rA(z)^2\cos(\gamma)\right]}{144}+\frac{r^2}{2}\left(\frac{r}{2}+\frac{1}{2}\right)\right.$$
$$\left.-ES_c\,r\left(\frac{A(z)^2}{4}-\frac{r^3}{12}-\frac{r^4}{48}\right)+S_cS_r\left[\frac{r^3E_cP_rH_r^2r^{2m-2}\left[U_{hs}\left(\left[\frac{I_0(\sqrt{m_0}\,r)}{I_0(\sqrt{m_0}\,A(z))}\right]-1\right)-\frac{\partial P}{\partial z}\left(\frac{A(z)^2-r^2}{4}\right)\left(M^2+\frac{1}{Z}\right)\right]^2}{Z^2}\right]+\ldots\right)$$

One of the most essential properties of blood flow is the wall shear stress, which can be found as follows:

$$S^{\bullet}_{zr}=\left(\frac{\partial w}{\partial r}\right)_{r=A(z)} \tag{23}$$

Shear stress can be expressed at the maximum stenosis height, i.e. at the throat stenosis at $z=a_1/b_1+1/n^{n/(n-1)}$ as:

$$\tau=\left(S^{\bullet}_{zr}\right)_{A(z)=1-\delta} \tag{24}$$

5. Convergence Analysis of YTHPM

In this section, we will study the convergence of analytical approximate solutions obtained from YTHPM for Equations (18-20), by depending on the convergence theorems that state: [35, 36]

Theorem (1): The analytical approximate solutions series $w=\sum_{k=0}^{\infty}w_k,\ T=\sum_{k=0}^{\infty}T_k$ and $C=\sum_{k=0}^{\infty}C_k$ obtained by YTHPM convergence if the following condition is fulfilled:

$$\|W_m-W_n\|\to 0 \quad \text{when} \quad n\to\infty,\ 0<\gamma<1\,.$$

Theorem (2): The new method (YTHPM) solutions $w=\sum_{k=0}^{\infty}w_k,\ T=\sum_{k=0}^{\infty}T_k$ and $C=\sum_{k=0}^{\infty}C_k$ converges and is close to the solution of problems (18-20) if the characteristic below is achieved:

$$L^{-1}N(w)=L^{-1}N(T)=L^{-1}N(C)=\lim_{m\to\infty}L^{-1}N(W_m),\quad \text{where} \quad L^{-1}(*)=\int_0^r(*)dr\,.$$

From these theorems and the resulting condition is defined as the following:

$$\gamma^m=\begin{cases}\dfrac{\|W_{m+1}-W_m\|}{\|W_1-W_0\|}=\dfrac{\|w_{m+1}\|}{\|w_1\|}=\dfrac{\|T_{m+1}\|}{\|T_1\|}=\dfrac{\|C_{m+1}\|}{\|C_1\|}, & \|w_1\|\neq 0,\|T_1\|\neq 0,\|C_1\|\neq 0,\quad m=1,2,3,\cdots\\ 0, & \|w_1\|=\|T_1\|=\|C_1\|=0.\end{cases}$$

We can analyze the convergence of solutions in the two cases as follows:
In the absence of the electro-osmotic field for velocity, temperature and concentration, respectively:

$$\|w_1 - w_0\| = \left\| \left[\frac{r^2 \sin\left(\frac{\gamma}{2}\right)^2 (G_m - G_r)\left(3A(z) - r^3 - \frac{r^4}{4}\right)}{12} - \frac{r^2 M^2 H_r \frac{\partial P}{\partial z}(m! r^{m+1})}{4} + \cdots \right] - \left(\left(\frac{r^2 - A(z)^2}{4} \right) \left(M^2 + \frac{1}{Z} \right) \frac{\partial P}{\partial z} \right) \right\|$$

$$\begin{aligned}
&\|w_2 - w_1\| \le \|w_1 - w_0\|\gamma, \quad \gamma = 0.000540 < 1,\\
&\|w_3 - w_2\| \le \|w_1 - w_0\|\gamma^2, \quad \gamma^2 = 0.00000925 < 1,\\
&\vdots\\
&\|w_m - w_{m-1}\| \le \|w_1 - w_0\|\gamma^m.
\end{aligned}$$

$$\|T_1 - T_0\| = \left\| \left[\left(\frac{\partial P}{\partial z}\right)^2 E_c P_r r \left[\frac{r^2 \sin\left(\frac{\gamma}{2}\right)^2 (G_m - G_r)(r^3 + 3r^2)}{12} - + \frac{r M^2 H_r \frac{\partial P}{\partial z}(m! r^{m+1})}{2} + \ldots \right] \right] - \left(\left(\frac{r^2 - A(z)^2}{4} \right) \right) \right\|$$

$$\begin{aligned}
&\|T_2 - T_1\| \le \|T_1 - T_0\|\gamma, \quad \gamma = 0.00433 < 1,\\
&\|T_3 - T_2\| \le \|T_1 - T_0\|\gamma^2, \quad \gamma^2 = 0.0000350 < 1,\\
&\vdots\\
&\|T_m - T_{m-1}\| \le \|T_1 - T_0\|\gamma^m.
\end{aligned}$$

$$\|C_1 - C_0\| = \left\| \left[\frac{\partial P}{\partial z}\left(\frac{r^2}{2}\left(\frac{r}{2} + \frac{1}{2} \right) + E S_c \left(\frac{A(z)^2}{4} - \frac{r^3}{12} - \frac{r^4}{48} \right) + \ldots \right) \right] - \left(\left(\frac{r^2 - A(z)^2}{4} \right) \right) \right\|$$

$$\begin{aligned}
&\|C_2 - C_1\| \le \|C_1 - C_0\|\gamma, \quad \gamma = 0.00995 < 1,\\
&\|C_3 - C_2\| \le \|C_1 - C_0\|\gamma^2, \quad \gamma^2 = 0.00000103 < 1,\\
&\vdots\\
&\|C_m - C_{m-1}\| \le \|C_1 - C_0\|\gamma^m.
\end{aligned}$$

In the presence of the electro-osmotic field for velocity, temperature and concentration, respectively:

$$\|w_1 - w_0\| = \left\| \left[-H_r \frac{r^2}{2} r^{m-1}(m+1) U_{hs} \left(\left[\frac{I_0(\sqrt{m_0}\, r)}{I_0(\sqrt{m_0}\, A(z))} \right] - 1 \right) + \cdots \right] - \left(\left(\frac{r^2 - A(z)^2}{4} \right) \left(M^2 + \frac{1}{Z} \right) \frac{\partial P}{\partial z} - U_{hs} \left(\left[\frac{I_0(\sqrt{m_0}\, r)}{I_0(\sqrt{m_0}\, A(z))} \right] - 1 \right) \right) \right\|$$

$$\begin{aligned}
&\|w_2 - w_1\| \le \|w_1 - w_0\|\gamma, \quad \gamma = 0.0000170 < 1,\\
&\|w_3 - w_2\| \le \|w_1 - w_0\|\gamma^2, \quad \gamma^2 = 8.523\text{E-}7 < 1,\\
&\vdots\\
&\|w_m - w_{m-1}\| \le \|w_1 - w_0\|\gamma^m.
\end{aligned}$$

$$\|T_1 - T_0\| = \left\| \left[\left(\frac{\partial P}{\partial z}\right)^2 \left[E_c P_r \frac{r^2}{2} \left(\left[M^2 + \frac{1}{Z} - \frac{H_r r^m}{Z} \right] \left[U_{hs} \left(\left[\frac{I_0(\sqrt{m_0}\, r)}{I_0(\sqrt{m_0}\, A(z))} \right] - 1 \right) \right] \right)^2 \right] + \cdots \right] - \left(\left(\frac{r^2 - A(z)^2}{4} \right) - S \left(\left[\frac{I_0(\sqrt{m_0}\, r)}{I_0(\sqrt{m_0}\, A(z))} \right] - 1 \right) \right) \right\|$$

$$\begin{aligned}
&\|T_2 - T_1\| \le \|T_1 - T_0\|\gamma, \quad \gamma = 0.00000845 < 1,\\
&\|T_3 - T_2\| \le \|T_1 - T_0\|\gamma^2, \quad \gamma^2 = 3.007\text{E-}12 < 1,\\
&\vdots\\
&\|T_m - T_{m-1}\| \le \|T_1 - T_0\|\gamma^m.
\end{aligned}$$

$$\|C_1 - C_0\| = \left\| \left[\frac{\partial P}{\partial z} \left(S S_c S_r r + E_c S_c S_r P_r M^4 r^3 \left[U_{hs} \left(\left[\frac{I_0(\sqrt{m_0}\, r)}{I_0(\sqrt{m_0}\, A(z))} \right] - 1 \right) \right]^2 + \ldots \right) \right] - \left(\left(\frac{r^2 - A(z)^2}{4} \right) \right) \right\|$$

$$\begin{aligned}
&\|C_2 - C_1\| \le \|C_1 - C_0\|\gamma, \quad \gamma = 0.00000140 < 1,\\
&\|C_3 - C_2\| \le \|C_1 - C_0\|\gamma^2, \quad \gamma^2 = 4.102\text{E-}11 < 1,\\
&\vdots\\
&\|C_m - C_{m-1}\| \le \|C_1 - C_0\|\gamma^m.
\end{aligned}$$

Through the analysis above, we notice the condition of convergence was attained in the cases of absence and presence electro-osmatic field. This is a proof of the effectiveness of the current method YTHPM in finding the analytical approximate solutions. Also it shows that the convergence theorems are applied successfully.

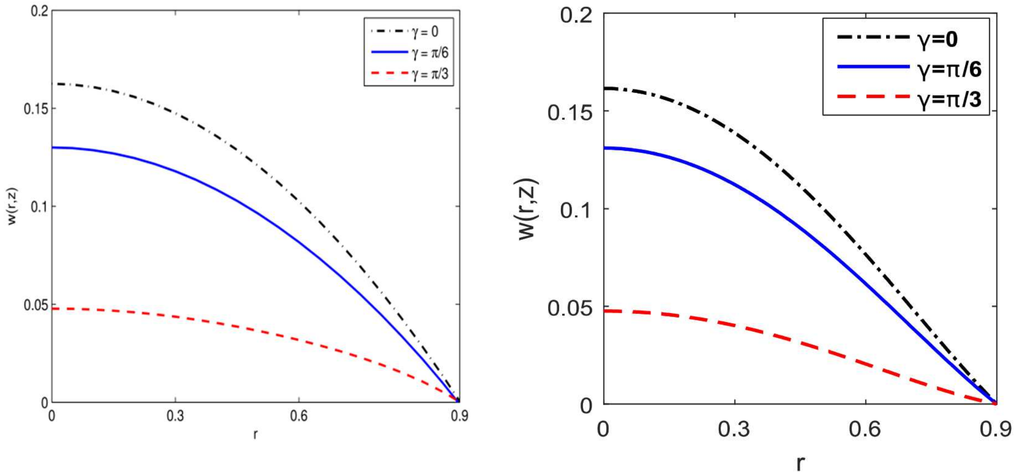

(a) (b)

Fig. 3. Comparison between (a) YTHPM and (b) Ref. [27] for the velocity at various values of γ.

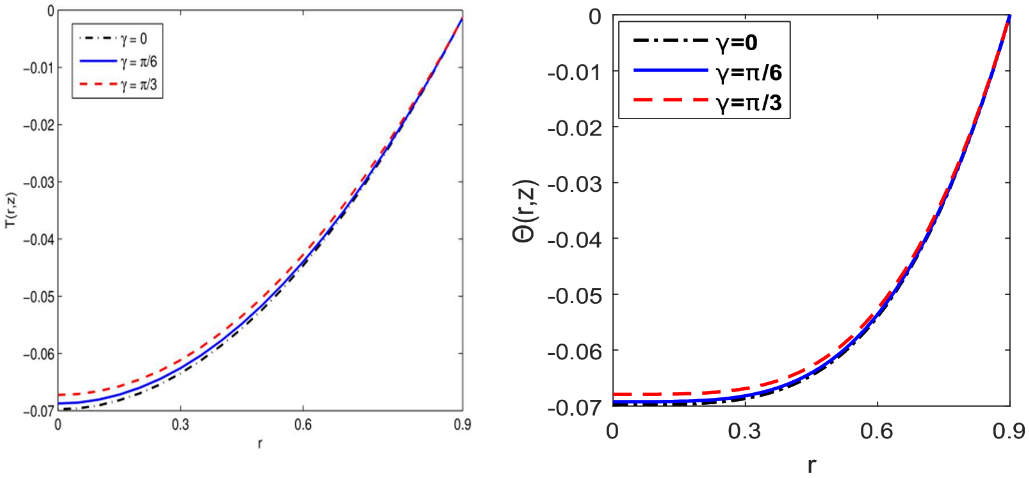

(a) (b)

Fig. 4. Comparison between (a) YTHPM and (b) Ref. [27] for the temperature at different values of γ.

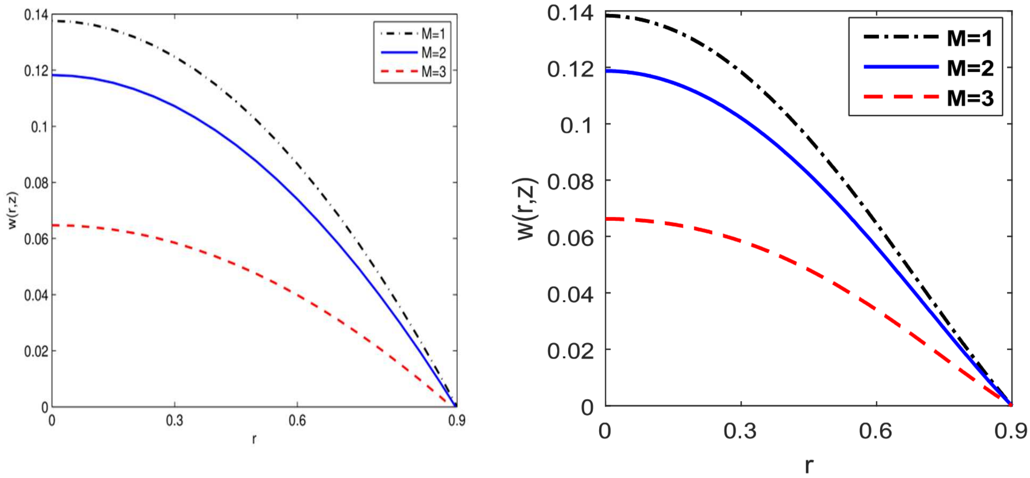

(a) (b)

Fig. 5. Velocity comparison between (a) YTHPM and (b) Ref. [27] at different values of M.

6. Results and Discussion

In this part, we will debate the results in two cases, the first in the absence of the effect of electro-osmosis (which considered as a comparison with Ref. [27]) and second with the presence of the effect of electro-osmosis (i.e., after the developments the problem).

Firstly, in the absence of the effect of electro-osmosis, as shown in the following:

Figure 3 explains the comparison of axial velocity between YTHPM and Ref. [27] at $n=2$, $S_r=0.5$, $S_c=1$, $\delta=0.1$, $z=1$, $G_m=2$, $G_r=3$, $\ell_1=0$, $E_c=2$, $P_r=1$ for various values of slant artery angle γ. We note from Fig. 3 that the velocity decreases when the slant angle of the artery increases, this shows that, at away from the center of the artery the velocity decreases in their maximum and at the stenosis wall of artery the velocity finally declines to zero. Figure 4 explains the comparison of temperature between YTHPM and Ref. [27] at the same values in Fig. 3 for various values of slant artery angle γ. It is noted that the slant artery angle has positive effect on the temperature, that is, when the angle slant of the artery increases, the temperature also increases.

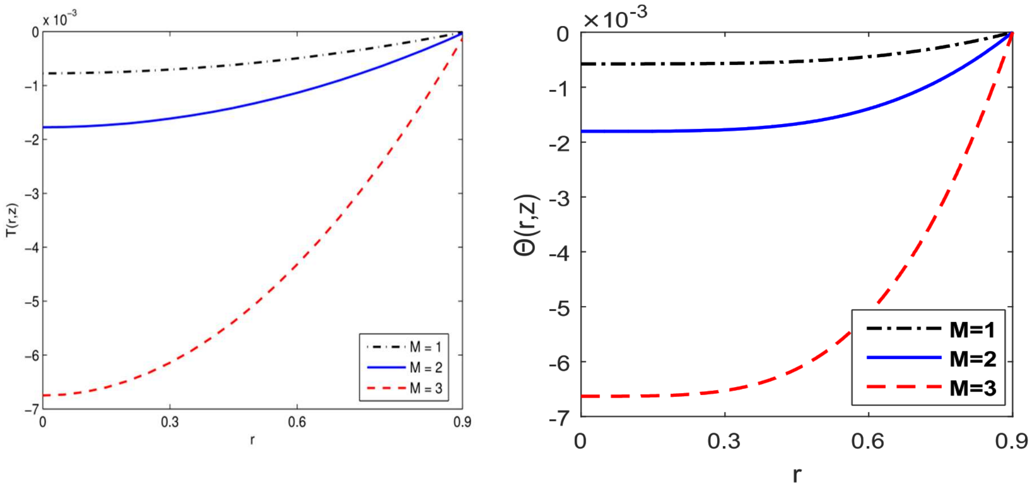

(a) (b)

Fig. 6. The compared of temperature for (a) YTHPM and (b) Ref. [27] at different values of M.

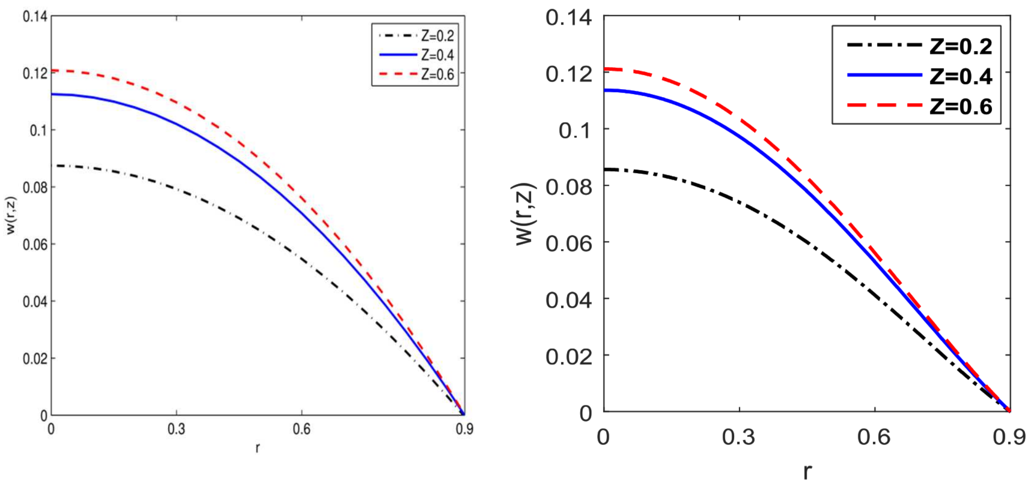

(a) (b)

Fig. 7. The axial velocity comparison between (a) YTHPM and (b) Ref. [27] at various values of Z.

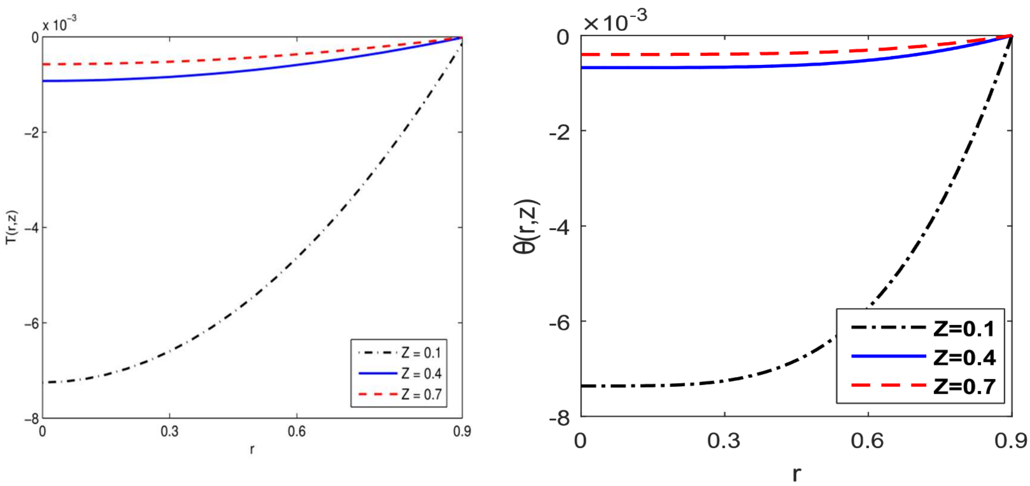

(a) (b)

Fig. 8. The temperature compared between (a) YTHPM and (b) Ref. [27] at various values of Z.

Figure 5 shows the comparison between YTHPM and Ref. [27] for velocity at the same values of parameter in Fig. 3 with various values of magnetic parameter M. It has been noticed that as the magnetic parameter increases, the velocity decreases. This happens due to the fact that blood contains magnetic iron oxide, and when a magnetic field impacts the blood, it feels a powerful electromotive power, which leads to the generation of a rotational movement of blood particles, and these impacts the speed of blood flow. Therefore, when the influence of the magnetic field increases, the Lorenz force which is stable amongst the applied magnetic field and the magnetic particles oppose the movement of the flow of blood and thus leads the blood velocity to decrease. As well, Fig. 6 illustrates the comparison between YTHPM and Ref. [27] for temperature at various values of the magnetic field. It's observed that the temperature also decreases when the value of M increases. This occurs due to the Lorentz force which dissents the movement of the flow of blood at the artery causing an increase in blood's internal viscosity, and due to the physical law of viscosity this leads to reduce the temperature value. As a result of the current research, it has been discovered that the body temperature can be controlled by applying an exterior magnetic field. This finding could be extremely beneficial in the treatment of cancer.

The effect of porosity parameter Z on axial velocity it shown in Fig. 7, which explains the velocity increase with the increase of Z. We note that the velocity in the middle of the artery reaches its maximum value; it begins to decrease towards the artery wall. This occurs due to a portion of the volume of the blanks increases over the total volume, and fluid particles get about from one venue to other in the artery. On the other hand, the temperature increases with the increase of Z as shown in Fig. 8 which illustrates the comparison between YTHPM and Ref. [27] for different values of porosity parameter Z on temperature. This can be explained physically as follows: as the porosity parameter increases, more area for heat to enter the fluid flow is created. As the temperature rises, so do the temperature profiles, which tend to rise as well.

The influence of chemical reaction parameter E on axial velocity as illustrated in Fig. 9, which explains the comparison between YTHPM and Ref. [27]. It is clear that the velocity increases when the chemical reaction parameter increases, which illustrates that E has positive effect on velocity. Furthermore, this figure shows that the velocity drops with a specified value of the chemical reaction parameter when one proceeds from the center of the artery towards stenated wall of arterial.

Secondly, in the presence of electro-osmosis, as shown in the following:

We demonstrated the impact of different slant angle with the influence of electro-osmotic parameter on the axial velocity as explained in Fig. 10. While in Fig. 11 clarifies the influence of Helmholtz Smoluchowski velocity on the axial velocity at various value of slant angle, it can be seen from Figs. 10 and 11 that when the slant angle decreases with the increase in m_0 and U_{hs} this leads to the velocity increase. This is because of the actuality that the flow increases with decreasing EDL thickness because of the reduction of fluid drag, so the bulk fluid moves relative to a charged surface because of, the exterior electrical field.

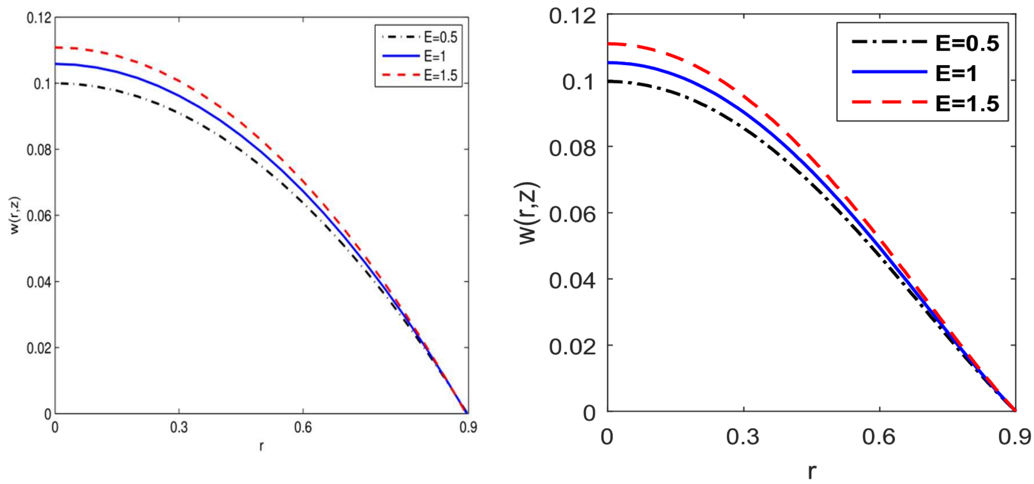

(a) (b)

Fig. 9. Comparison between (a) YTHPM and (b) Ref. [27] for the axial velocity at different values of E.

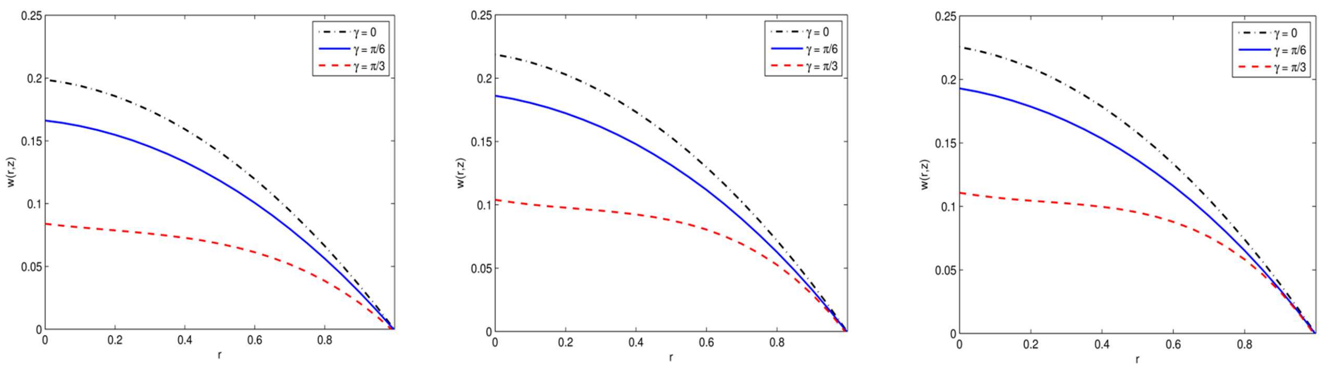

$m_0 = 2$ $m_0 = 4$ $m_0 = 5$

Fig. 10. Impact of electro-osmotic parameter (m_0) on the axial velocity at various values of γ and $U_{hs} = 0.1$.

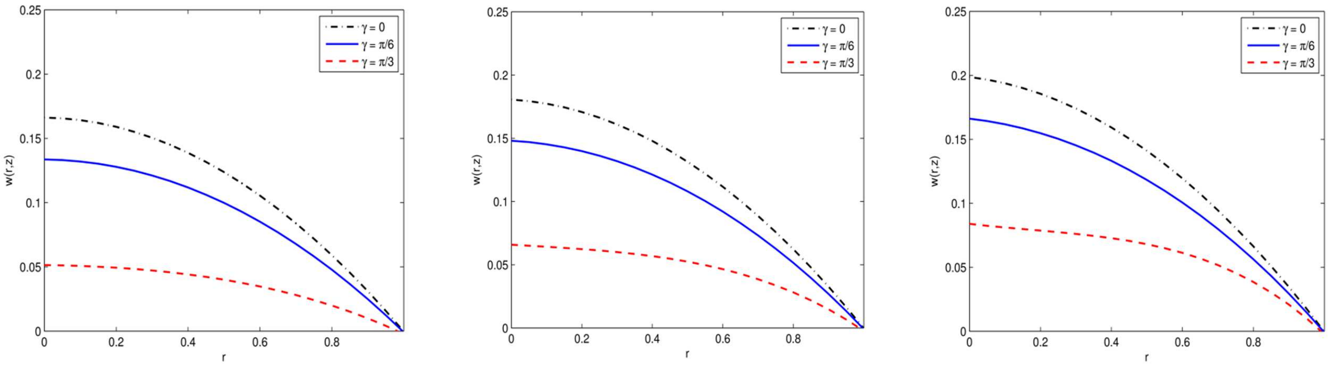

$U_{hs} = 0.01$ $U_{hs} = 0.05$ $U_{hs} = 0.1$

Fig. 11. Impact of Helmholtz Smoluchowski velocity (U_{hs}) on the axial velocity at various values of γ and $m_0 = 2$.

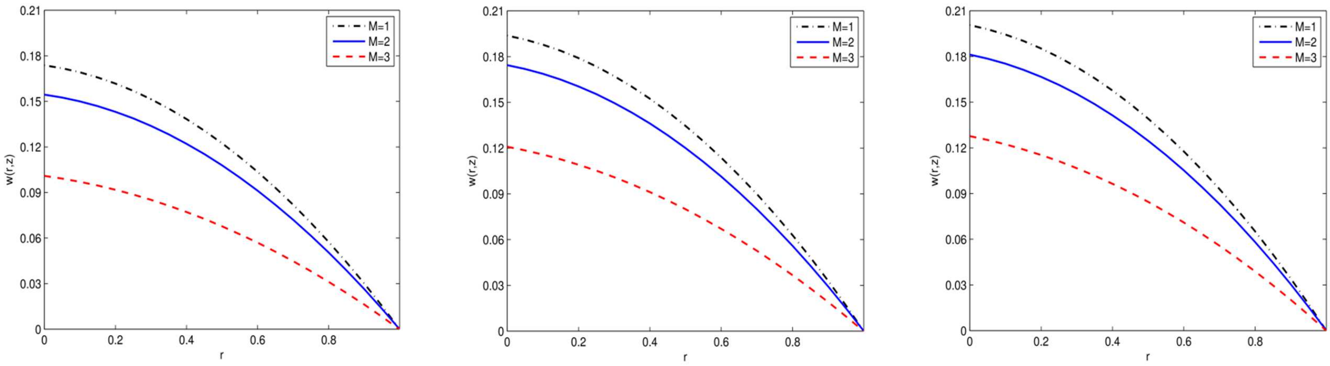

$m_0 = 2$ $m_0 = 4$ $m_0 = 5$

Fig. 12. Influence of electro-osmotic parameter (m_0) on the axial velocity at various values of M and $U_{hs} = 0.1$.

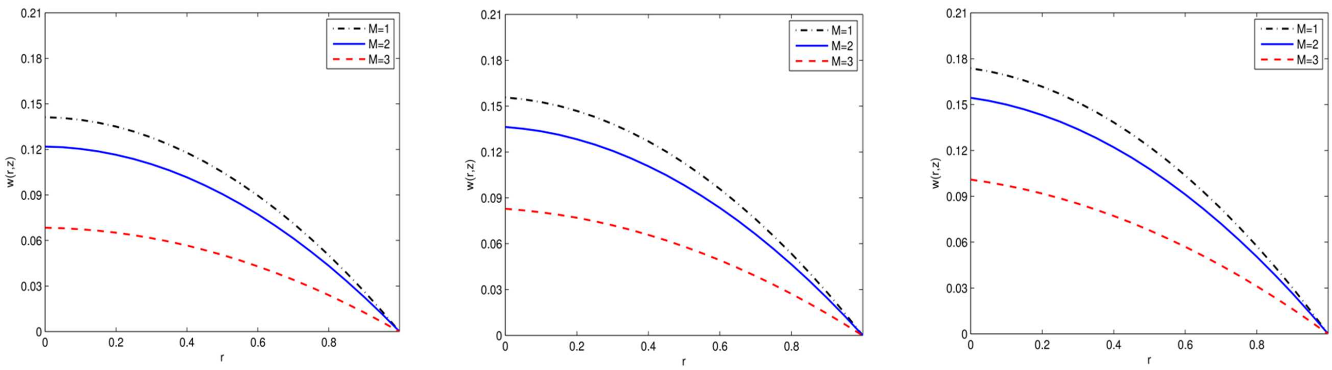

$U_{hs} = 0.01$ $U_{hs} = 0.05$ $U_{hs} = 0.1$

Fig. 13. Impact of Helmholtz Smoluchowski velocity (U_{hs}) on the axial velocity at various values of M and $m_0 = 2$.

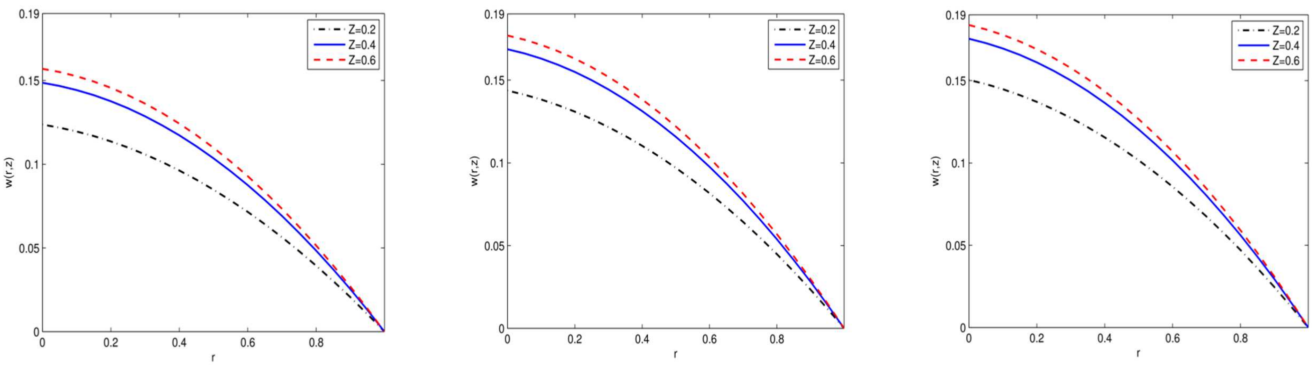

$m_0 = 2$ $m_0 = 4$ $m_0 = 5$

Fig. 14. Influence of electro-osmotic parameter (m_0) on the axial velocity at various values of Z and $U_{hs} = 0.1$.

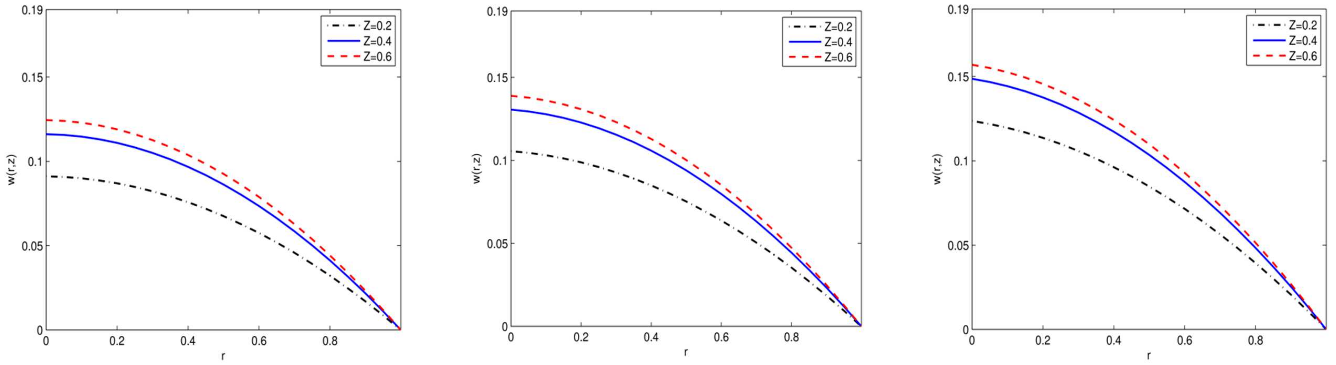

$U_{hs} = 0.01$ $U_{hs} = 0.05$ $U_{hs} = 0.1$

Fig. 15. Impact of Helmholtz Smoluchowski velocity (U_{hs}) on the axial velocity at various values of Z and $m_0 = 2$.

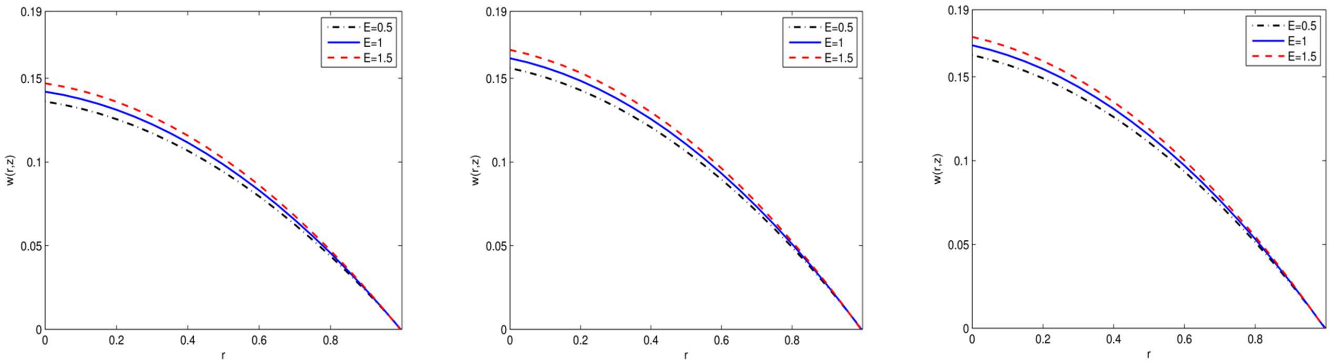

$m_0 = 2$ $m_0 = 4$ $m_0 = 5$

Fig. 16. Influence of electro-osmotic parameter (m_0) on the axial velocity at various values of E and $U_{hs} = 0.1$.

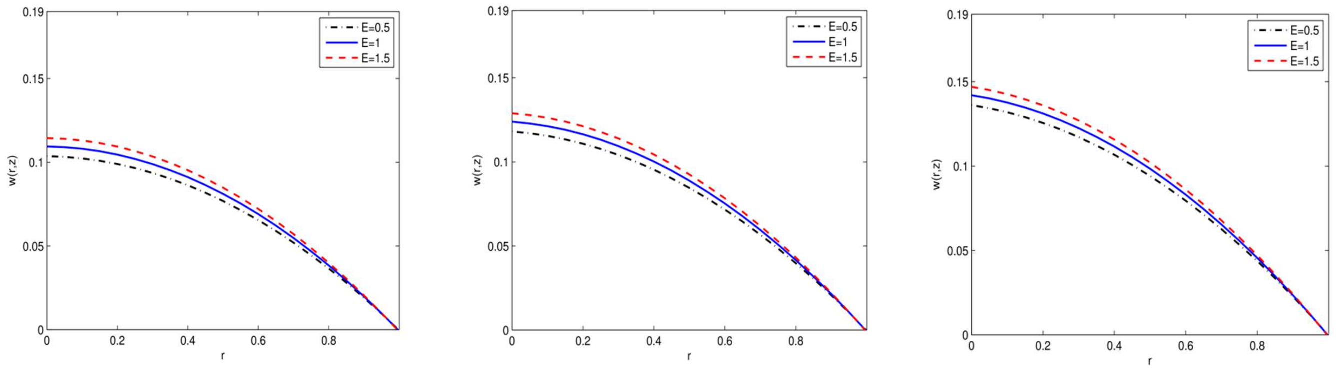

$U_{hs} = 0.01$ $U_{hs} = 0.05$ $U_{hs} = 0.1$

Fig. 17. Effect of Helmholtz Smoluchowski velocity (U_{hs}) on the axial velocity at various values of E and $m_0 = 2$.

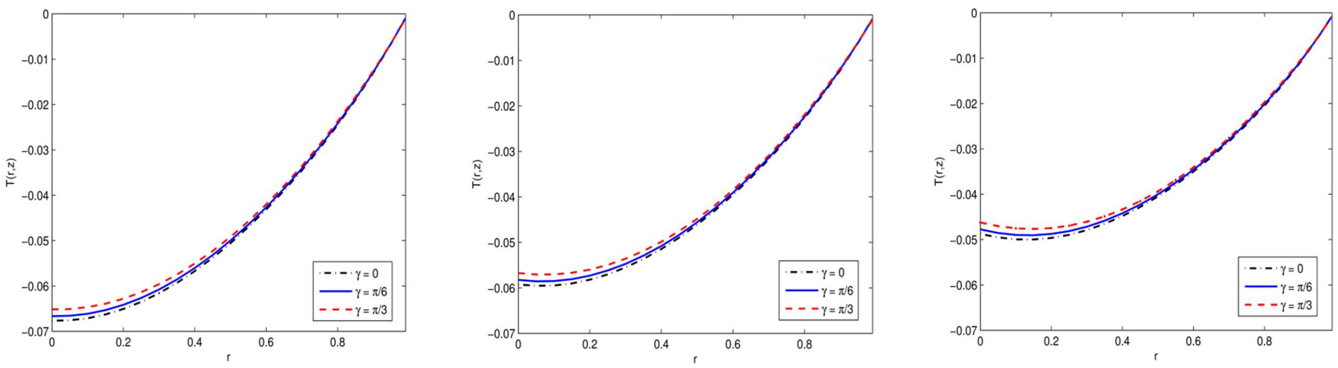

$S = 0.01$ $S = 0.05$ $S = 0.1$

Fig. 18. Impact of Joule heating (S) on the temperature at various values of γ, $m_0 = 1$ and $U_{hs} = 0.1$.

Whilst, Figs. 12 and 13 illustrate the impact of the electro-osmotic parameter and Helmholtz Smoluchowski velocity on the axial velocity with different values of M, we note that when increasing the m_0 and U_{hs} with decreasing magnetic field, this leads to the velocity increase. This means that m_0 and U_{hs} has positive influence on velocity, while they have an opposite impact with magnetic field, this is due to the Lorentz force which dissents the movement of the flow of blood and that leads to the blood velocity to decrease.

Moreover; Figs. 14 and 15 show the influence of the electro-osmotic parameter and Helmholtz Smoluchowski velocity on the axial velocity, respectively. It can be seen from Figs. 14 and 15 that when increasing the porosity parameter with increasing in m_0 and U_{hs} then the velocity also increases. This implies a strong electrical field, and because the U_{hs} is directly proportional to the electric field, this leads to an increase in velocity. Furthermore, because Debye length is inversely linked to m_0, raising the electro-osmotic parameter causes Debye length to decrease, resulting in an increase in velocity.

Moreover, Figs. 16 and 17 illustrate the effect of E together with the impact of m_0 and U_{hs} on the axil velocity. It is clear that the velocity increases when the chemical reaction parameter increases with increasing m_0 and U_{hs}. This means that the joint effects of E, m_0 and U_{hs} are directly proportional with the velocity.

Furthermore; Fig. 18 shows the impact of Joule heating parameter (S) on temperature profile at different values of γ. Notes that the temperature increases with the increase of S and γ, i.e. S and γ has a positive effect on the temperature. The impact of Joule heating parameter (S) on temperature profile at various values of M it can be seen in Fig. 19, which illustrates that the temperature decreases when S increases with increasing M, because of the Lorentz force which causes an increase in blood's internal viscosity this leads to reduce the temperature value. Besides Fig. 20 explains the influence of the Joule heating parameter (S) on temperature profile at different values of Z. It has been noted that temperature increases with increasing S and increasing Z, and this is due to more space for heat is created to enter the fluid flow when Z increase. So, as the temperature increases, the temperature profiles also increase. And because of the Joule heating is a crucial process of electro-osmotic flow that determines the amount of heat created by an electric current, as a result, the electric field is primarily responsible for heat transfer with fluid speed. This means that temperature is highly influenced by Joule heating.

Now, we illustrate the concentration in two cases absence and presence electro-osmotic as follows:

It can be seen when that increase the magnetic field the concentration for the blood flow decrease, as shown in Fig. 21 which illustrates the YTHPM solutions (in absence and presence of electro-osmotic) and Ref. [27] for concentration at various value of M. We see also the electro-osmotic on concentration has no significant effect. Further, Fig. 22 demonstrates the YTHPM (in absence and presence of electro-osmotic) and Ref. [27] for concentration at different values of Z. Note that the concentration increase as increase Z. This due to the fact when the porosity parameter increases, this gives an area for greater heat input to fluid flow. The increasing heat also affects the temperature profile and tends to increase and also raises the concentration.

Moreover; the influence of chemical reaction parameter E on concentration (in absence and presence electro-osmotic) shown in Fig. 23, which explains the comparison between YTHPM and Ref. [27]. It is clear that the concentration increases when the chemical reaction parameter increases. We notice that, the concentration profile reaches a peak in the center of the artery by following the parabolic course, then begins to decline towards the core region's interface, eventually reaching zero at the outer wall. In all comparison figures, we note that there is an excellent agreement with the previous study [27] in the state absence of electro-osmotic.

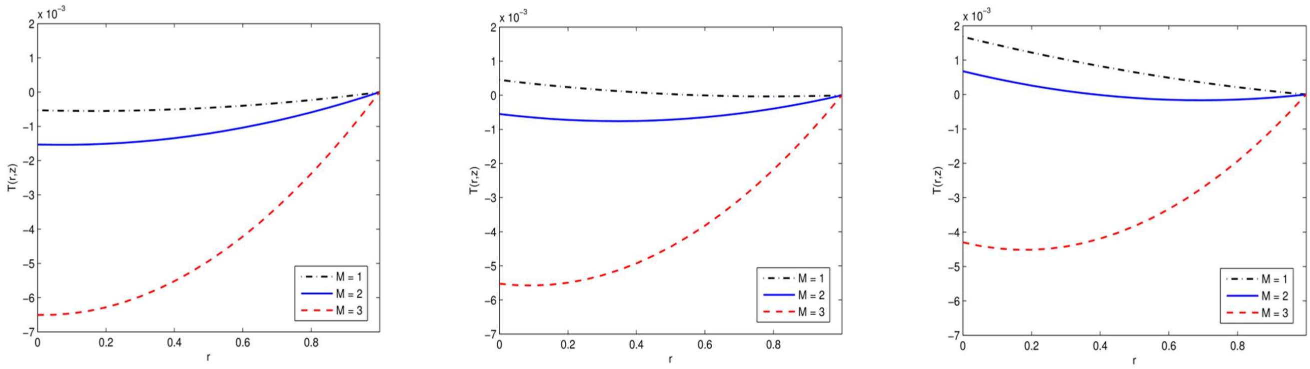

S = 0.01 S = 0.05 S = 0.1

Fig. 19. Influence of Joule heating (S) on the temperature at various values of M, $m_0 = 0.1$ and $U_{hs} = 0.1$.

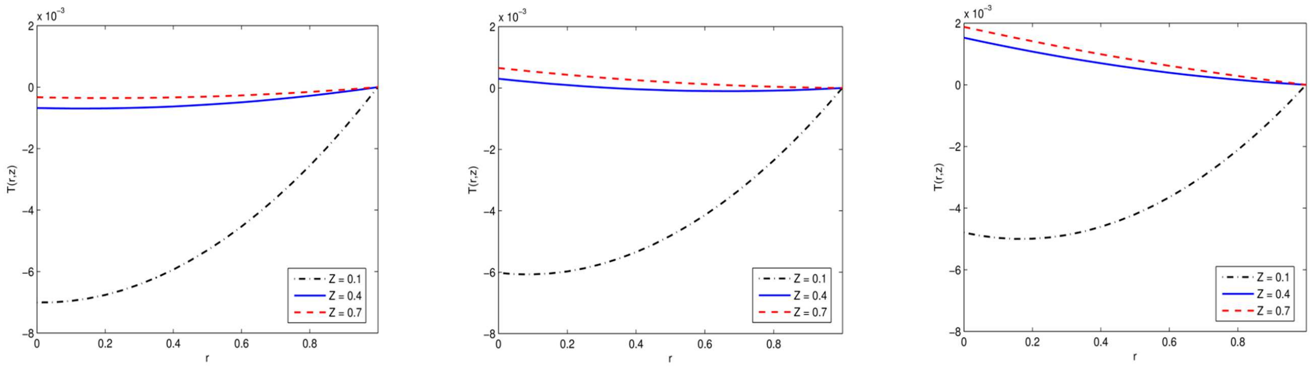

S = 0.01 S = 0.05 S = 0.1

Fig. 20. Effect of Joule heating (S) on the temperature at various values of Z, $m_0 = 0.1$ and $U_{hs} = 0.1$.

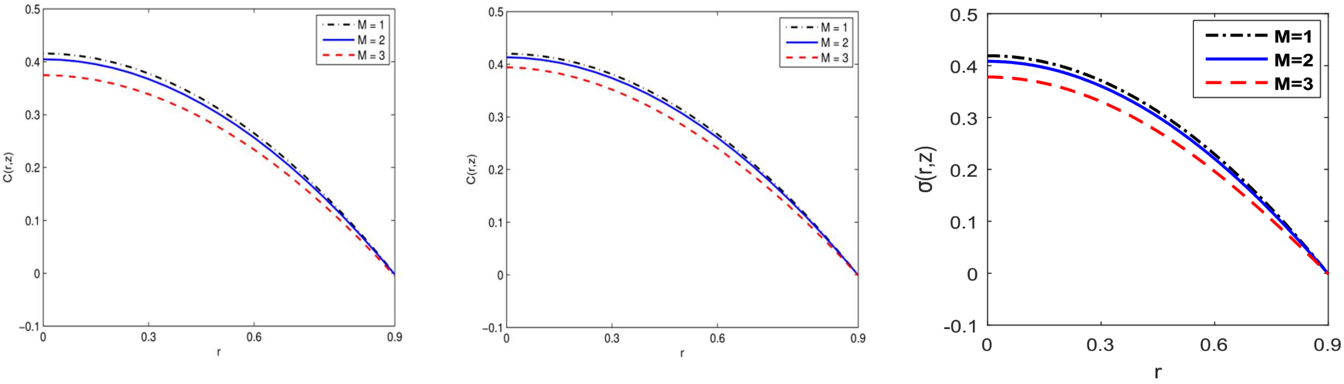

(a) (b) (c)

Fig. 21. YTHPM (a): absence electro-osmotic, (b): presence electro-osmotic and (c): Ref. [27], for concentration at various values of M.

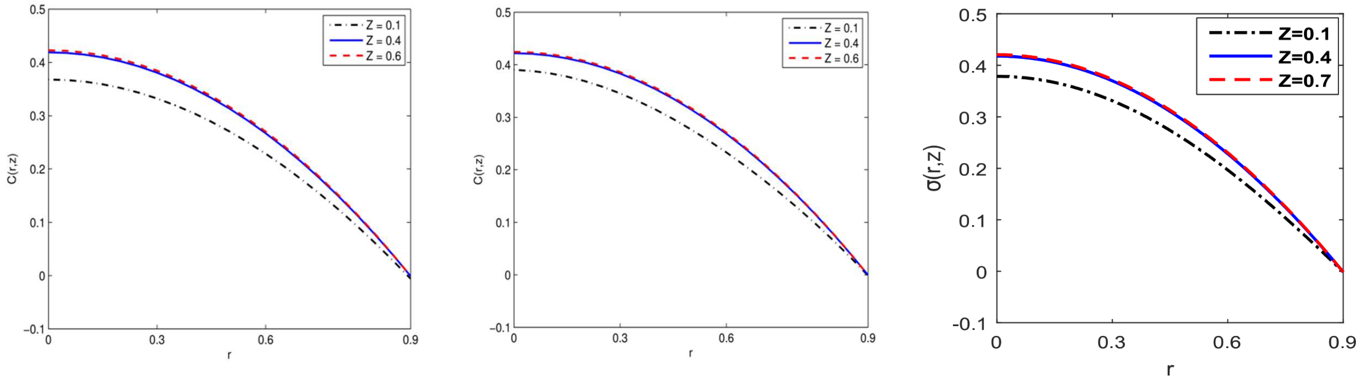

(a) (b) (c)

Fig. 22. YTHPM (a): absence electro-osmotic, (b): presence electro-osmotic and (c): Ref. [27], for concentration at various values of Z.

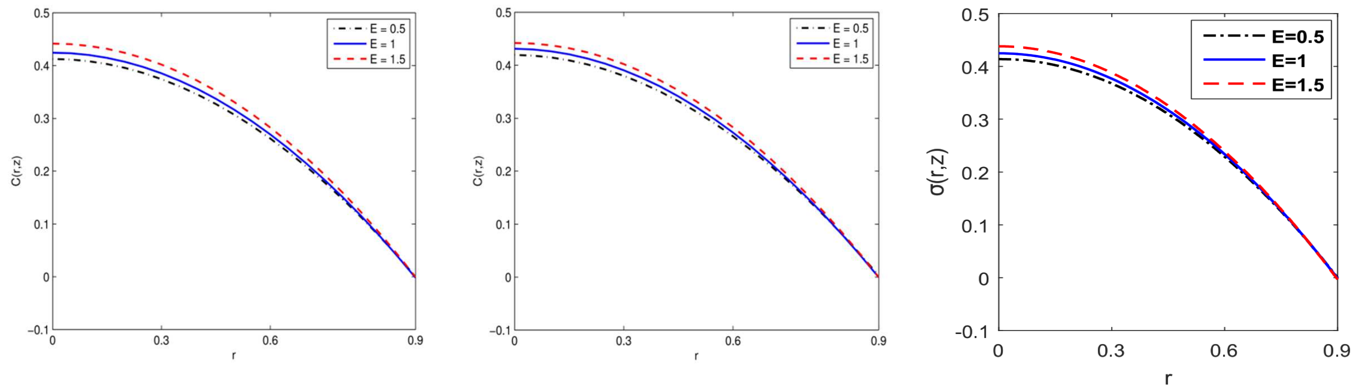

(a) (b) (c)

Fig. 23. Comparison between YTHPM (a): absence electro-osmotic, (b): presence electro-osmotic, (c): Ref. [27] for concentration at various values of E.

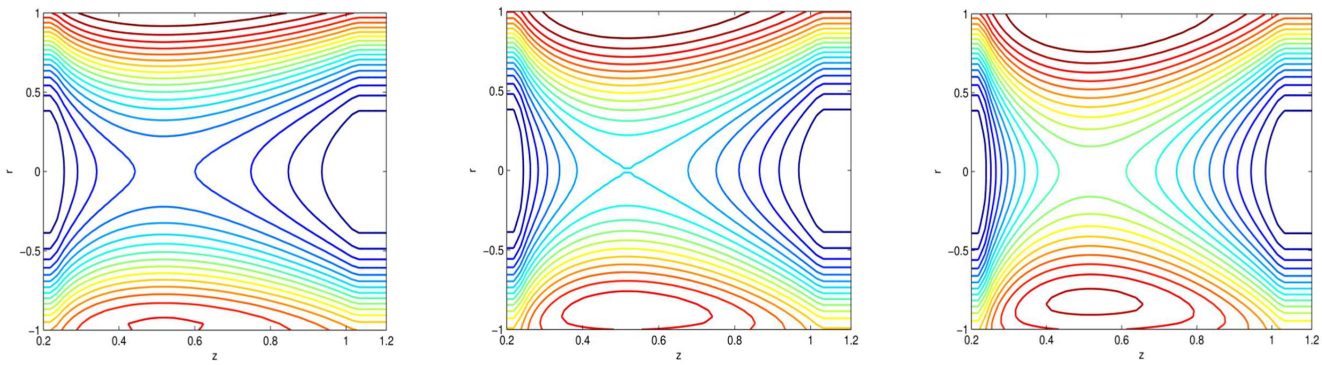

$\delta = 0.1$ $\delta = 0.15$ $\delta = 0.2$

Fig. 24. Velocity contour plot for various values of height stenosis at ($\delta = 0.1$, $\delta = 0.15$ and $\delta = 0.2$) respectively, for case absence of electro-osmotic.

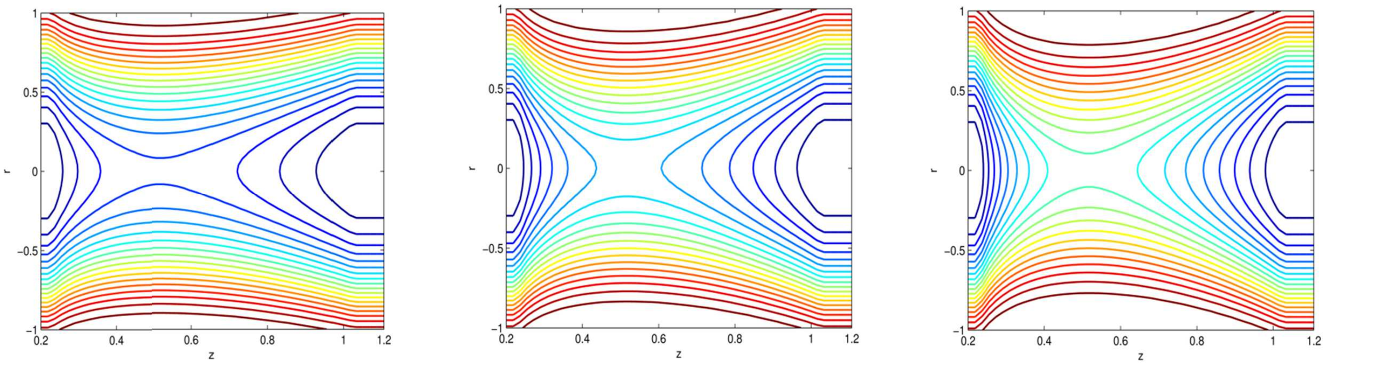

$\delta = 0.1$ $\delta = 0.15$ $\delta = 0.2$

Fig. 25. Velocity contour plot for various values of height stenosis at ($\delta = 0.1$, $\delta = 0.15$ and $\delta = 0.2$) respectively, for case presence of electro-osmotic.

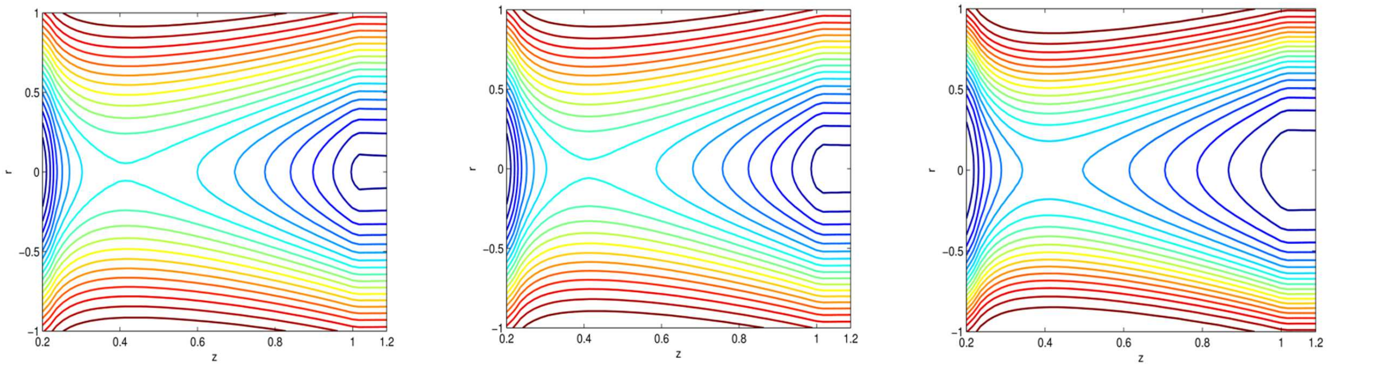

$M = 1$ $M = 2$ $M = 3.5$

Fig. 26. Velocity contour plot for various values of magnetic field ($M = 1, 2, 3.5$) respectively, for case absence of electro-osmotic.

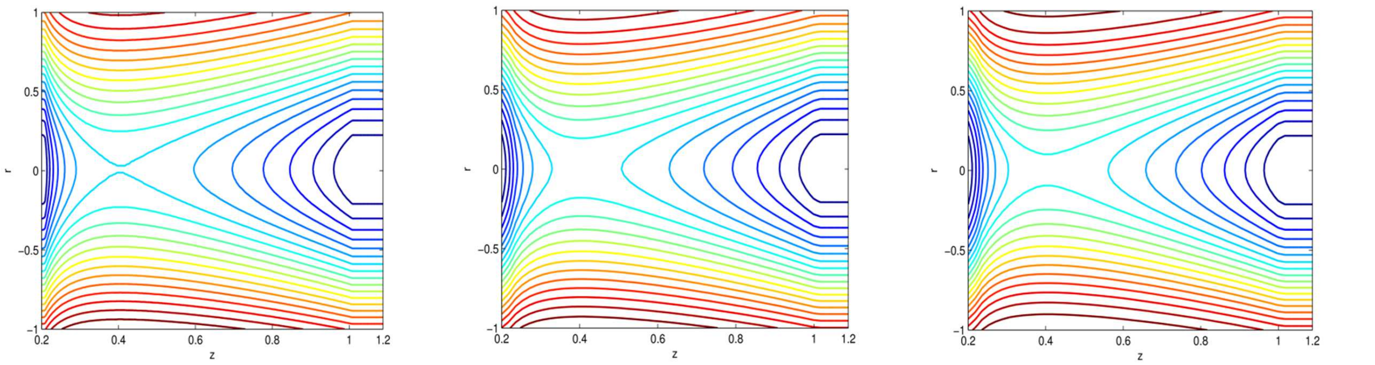

$M = 1$ $M = 2$ $M = 3.5$

Fig. 27. Velocity contour plot for various values of magnetic field ($M = 1, 2, 3.5$) respectively, for case presence of electro-osmotic.

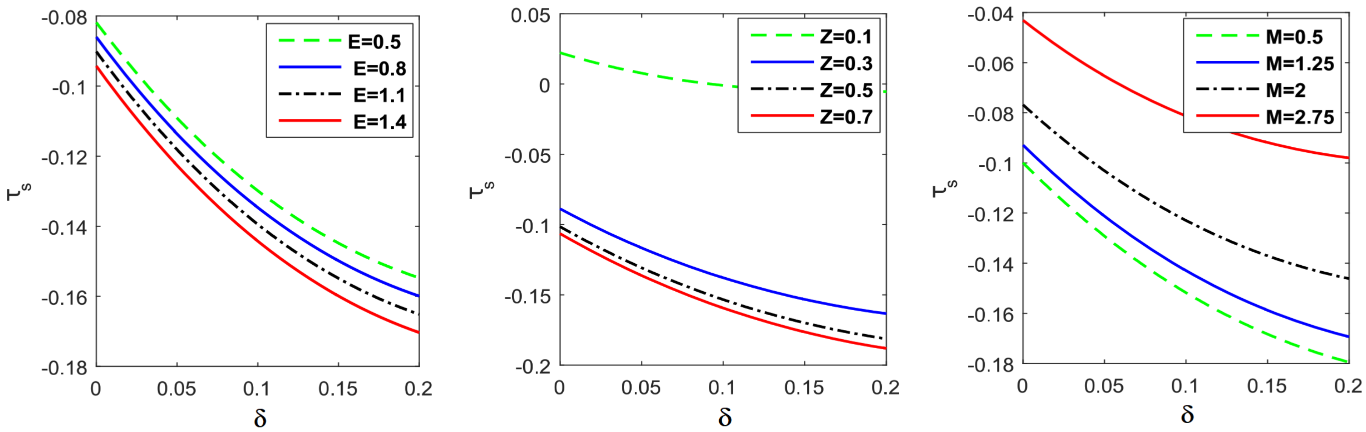

(a)

Fig. 28. Wall shear stress comparison between (a) Ref. [27] and (b) YTHPM at various values of E, Z, M respectively.

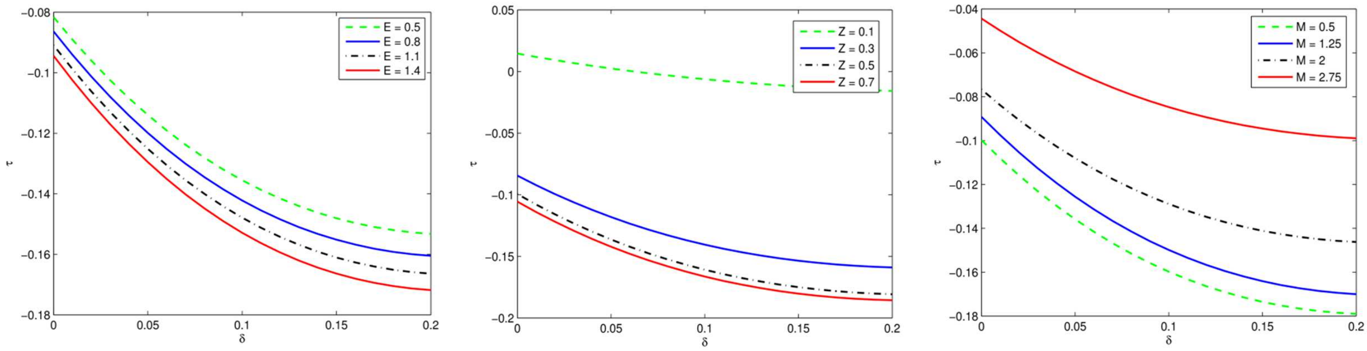

(b)

Fig. 28. Continued.

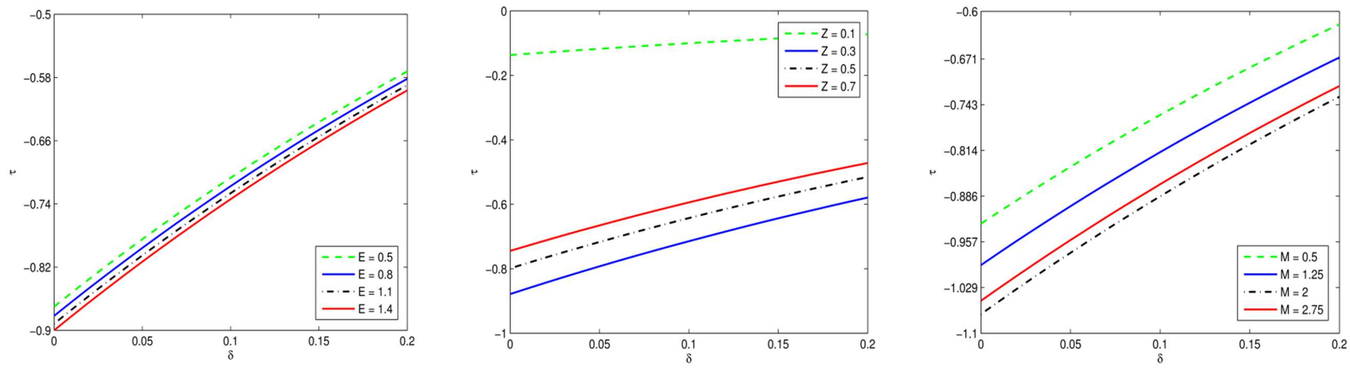

Fig. 29. Wall shear stress with the effect of electro-osmotic parameter $m_0 = 1$ for YTHPM for different values of E, Z, M respectively, and $U_{hs} = 0.1$.

Figures 24 and 25 show the comparison for contour velocity for YTHPM solutions for two states in absence and presence the effect of electro-osmotic for different values of height stenosis (δ = 0.1, 0.15, 0.2). Moreover; Figs. 26 and 27 explain the comparison for contour velocity for YTHPM solutions for two state absence and presence the effect of electro-osmotic for various values of magnetic parameter (M = 1, 2, 3). We can see that as the stenosis height grows, the size of the trapped bolus grows as well, slowing blood flow progressively at stenosis maximum height. Additionally, as M increases, the trapped bolus grows in size, reducing the blood flow velocity progressively.

Figure 28 illustrates the wall shear stress at various values of E, Z and M, respectively. From this figure, it is observed that the wall shear stress decreases when E, Z increases, while its increase with increasing M. High magnetic field intensities can trigger rupture of a plaque, which can harm the body by paralyzing the affected area. Finally, Fig. 29 demonstrates the effect of electro-osmotic ($m_0 = 1,\ U_{hs} = 0.1$) on wall shear stress at different values of E, Z and M, respectively. We note the wall shear stress has different behavior with existing the effect of electro-osmotic field. Thermo- physical properties of Blood used in this research are presented in Table 1.

Table 1. Thermo- physical properties of Blood [37].

Property	Blood
Specific heat ($J/kg.K$)	3594
Density (kg/m^3)	1063
Thermal conductivity ($W/m.K$)	0.492

7. Conclusions

In this paper, the developed model of blood flow in an oblique artery with mild stenosis under the effect of the magnetic field, electro-osmotic, chemical reaction, porosity and variable viscosity was studied using the Yang transform homotopy perturbation method (YTHPM), which is considered as an expansion for the application of YTHPM proposed in [35, 36]. The results obtained from YTHPM for solving the developed model presented in Ref. [27] (i.e. by adding the effect of electro-osmotic) illustrate the following:

• An increase in m_0 and U_{hs} with a decrease of γ, M and increasing Z, E leads to the velocity increases.
• An increase in Joule heating with increasing γ, M, Z rises the temperature increase at constant values of m_0 and U_{hs}.
• It was noted that the electro-osmotic on concentration has no significant effect.
• It was concluded through the convergence analysis that the obtained solutions using YTHPM in the presence of the electro-osmotic field are faster converged compared to the absence of the field, and this in turn leads to the values of the error being small.
• Moreover, the results affirmed the ability and validity of the new method to solve the problem and excellent agreement were found by comparing with the previous results.
• Furthermore; this study showed the importance of applying electro-osmotic by the transfer of medication and reducing the risk of diseases through proper use which can benefit physicians during the surgical operations.
• It was concluded that YTHPM is a powerful, easy and effective method for locating analytical approximate solutions to the current problem which can be applied on more complex flow problems with real-world applications.

Author Contributions

T.A.J. Al-Griffi has developed the mathematical model for the current problem as well as the methodology in addition to the formal analysis, data processing, investigation, software and writing the original draft of the current paper as well as reviewing and editing it. A.S.J. Al-Saif supervised the study and studied the presented methodology as well as reviewed and edited the current version of the paper.

Acknowledgments

Not applicable.

Conflict of Interest

The authors declared no potential conflicts of interest concerning the research, authorship, and publication of this article.

Funding

The authors received no financial support for the research, authorship, and publication of this article.

Data Availability Statements

The datasets generated and/or analyzed during the current study are available from the corresponding author on reasonable request.

Nomenclature

YTHPM	Yang transform homotopy perturbation method.
EOF	Electro-osmotic flow.
EDL	The electrical double layer.
DTM	Differential transform method.
$\hat{u}, \hat{v}, \hat{w}$	The components of velocity in $\hat{r}, \hat{\theta}, \hat{z}$ trends.
$L(\hat{C}-\hat{C}_0)$	The chemical reaction parameter factor.
σ^*	The electrical conductivity.
κ^*	The thermal diffusion.
$k_1^\bullet$	The permeability of pored midst.
μ_{m1}	The permeability of magnetic.
$\hat{C}$	The mass concentricity.
$\hat{T}$	The temperature.
$\hat{P}$	The pressure.
c_p	The specific heat.
D	The ratio of thermal-diffusion.
K_T	The mass diffusivity coefficients.
T_m	The medium's temperature.
S	The Joule heating.
$\rho_e^\bullet$	The net of the charge density.
$E^\bullet$	The electric field.
H	The maximum hematocrit in the artery center.
H_r	The parameter of hematocrit.
d_0	The non-tapered artery radius.
ϕ	The tapering angle.
$\delta^\bullet$	The stenosis height.
n	The parameter that defines the form for the stenosis.
i_e	The current density.
$\hat{\Phi}$	The function of electro-osmotic potential.
ℓ^*	The dielectric constant.
n^-, n^+	The negative and positive ions.
e	The charge electronic.
$z^\bullet$	The charge balance.
ς	Zeta potential.
I_0	The modulation Bessel function for the first type of order zero.
m_0	The electro-osmotic parameter.
u_0	The velocity average of flow in a regular artery.
$\hat{C}_0$ and $\hat{T}_0$	The concentration of mass and average temperature.
S_c, S_r, E_c, Pr, Re	The Schmidt, Soret, Eckert, Prandtl, Reynolds numbers.
M, E, λ_d^*	The magnetic parameter, chemical reaction parameter, Debye-Length.
U_{hs}	The Helmholtz Smoluchowski velocity.
Z	The porosity parameter.

References

[1] Ali, N., Zaman, A., Sajid, M., Unsteady blood flow through a tapered stenotic artery using Sisko model, *Computers & Fluids*, 101, 2014, 42–49.
[2] Mandal, P.K., Chakravarty, S., Mandal, A., Amin, N., Effect of body acceleration on unsteady pulsatile flow of non-newtonian fluid through a stenosed artery, *Applied Mathematics and Computation*, 189, 2007, 766–779.
[3] Chakravarty, S., Mandal, P.K., A nonlinear two-dimensional model of blood flow in an overlapping arterial stenosis subjected to body acceleration, *Mathematical and Computer Modelling*, 24(1), 1996, 43-58.
[4] Srivastava, V.P., Rastogi, R., Vishnoi, R., A two-layered suspension blood flow through an overlapping stenosis, *Computers & Mathematics with Applications*, 60, 2010, 432–441.
[5] Zaman, A., Ali, N., Sajid, M., Hayat, T., Effects of unsteadiness and non-Newtonian rheology on blood flow through a tapered time-variant stenotic artery, *AIP Advances*, 5, 2015, 037129.
[6] Ikbal, Md., A., Chakravarty, S., Wong, K.K.L., Mazumdar, J., Mandal, P.K., Unsteady response of non-Newtonian blood flow through a stenosed artery in magnetic field, *Journal of Computational and Applied Mathematics*, 230, 2009, 243–259.
[7] Varshney, G., Katiyar, V.K., Kumar, S., Effect of magnetic field on the blood flow in artery having multiple stenosis: a numerical study, *International Journal of Engineering, Science and Technology*, 2(2), 2010, 67-82.
[8] Siddiqui, S.U., Geeta, A mathematical model for blood flow through inclined stenosed artery, *International Journal of Mathematics and its Applications*, 4, 2016, 189–195.
[9] Chitra, M., Karthikeyan, D., Unsteady MHD oscillatory blood flow in an inclined tapered artery with mild stenosis through porous medium: effects of slip velocity, *International Journal of Mathematics Trends and Technology*, Special Issue NCCFQET, 2018, 44-49.

[10] Akram, S., Aly, E.H., Afzal, F., Nadeem, S., Effect of the variable viscosity on the peristaltic flow of newtonian fluid coated with magnetic field: application of adomian decomposition method for endoscope, *Coatings*, 9, 2019, 524.
[11] Abo-Elkhair, R.E., Mekheimer, Kh.S., Moawad, A.M.A., Combine impacts of electrokinetic variable viscosity and partial slip on peristaltic MHD flow through a micro-channel, *Iranian Journal of Science and Technology, Transactions A: Science*, 43, 2017, 201–212.
[12] Coccarelli, A., Prakash, A., Nithiarasu, P., A novel porous media based approach to outflow boundary resistances of 1D arterial blood flow models, *Biomechanics and Modeling in Mechanobiology*,18, 2019, 939–951.
[13] Govindaraju, K., Kamangar, S., Badruddin, I.A., Viswanathan, G., N., Badarudin, A., Ahmed, N., J., S., Effect of porous media of the stenosed artery wall to the coronary physiological diagnostic parameter: A computational fluid dynamic analysis, *Atherosclerosis*, 233, 2014, 630-635.
[14] Akbar, N.S., Nadeem, S., Influence of heat and chemical reactions on the Sisko fluid model for blood flow through a tapered artery with a mild stenosis, *Quaestiones Mathematicae*, 37(2), 2014, 157-177.
[15] Mekheimer, Kh.S., Haroun, M.H., El Kot, M.A., Influence of heat and chemical reactions on blood flow through an anisotropically tapered elastic arteries with overlapping stenosis, *Applied Mathematics & Information Sciences*, 6(2), 2012, 281-292.
[16] Mwapinga, A., Mureithi, E., Makungu, J., Masanja, V., MHD arterial blood flow and mass transfer under the presence of stenosis, body acceleration and chemical reaction: a case of magnetic therapy, *Journal of Mathematics and Informatics*, 18, 2020, 85-103.
[17] Misra, J.C., Adhikary, S.D., MHD oscillatory channel flow, heat and mass transfer in a physiological fluid in presence of chemical reaction, *Alexandria Engineering Journal*, 55, 2016, 287–297.
[18] Saleem, S., Akhtar, S., Nadeem, S., Saleem, A., Ghalambaz, M., Issakhov, A., Mathematical study of Electroosmotically driven peristaltic flow of Casson fluid inside a tube having systematically contracting and relaxing sinusoidal heated walls, *Chinese Journal of Physics*,71, 2021, 300-311.
[19] Ponalagusamy, R., Manchi, R., Particle–fluid two phase modeling of electro-magneto hydrodynamic pulsatile flow of Jeffrey fluid in a constricted tube under periodic body acceleration, *European Journal of Mechanics - B/Fluids*, 81, 2020, 76–92.
[20] Abdelsalam, S.I., Mekheimer, Kh.S., Zaher, A.Z., Alterations in blood stream by electroosmotic forces of hybrid nanofluid through diseased artery: Aneurysmal/stenosed segment, *Chinese Journal of Physics*, 67, 2020, 314–329.
[21] Tripathi, D., Bhushan, S., Be´g, O.A., Unsteady viscous flow driven by the combined effects of peristalsis and electro-osmosis, *Alexandria Engineering Journal*, 57, 2018, 1349–1359.
[22] Moatimid, G.M., Mohamed, M.A.A., Hassan, M.A., El-Dakdoky, E.M.M., Electro-osmotic flow and heat transfer of a non-Newtonian nanofluid under the influence of peristalsis, *Pramana - Journal of Physics*, 92, 2019, 90.
[23] Mondal, A., Shit, G.C., Transport of magneto-nanoparticles during electro-osmotic flow in a micro-tube in the presence of magnetic field for drug delivery application, *Journal of Magnetism and Magnetic Materials*, 442, 2017, 319-328.
[24] Tripathi, B., Sharma, B.K., MHD blood flow and heat transfer through an inclined stenosed artery with variable viscosity, arXiv:1610.03470v2 [physics.flu-dyn] 28 May 2017, 2017, 1-15.
[25] Tripathi, B., Sharma, B.K., Effect of heat transfer on MHD blood flow through an inclined stenosed porous artery with variable viscosity and heat source, *Romanian Journal of Biophysics*, 28(3), 2018, 89–102.
[26] Tripathi, B., Sharma, B.K., Influence of heat and mass transfer on two-phase blood flow with Joule heating and variable viscosity in the presence of variable magnetic field, *International Journal of Computational Methods*, 17(3), 2018, 1-21.
[27] Tripathi, B., Sharma, B.K., Effect of variable viscosity on MHD inclined arterial blood flow with chemical reaction, *International Journal of Applied Mechanics and Engineering*, 23(3), 2018, 767-785.
[28] Abubakar, J.U., Adeoye, A.D., Effects of radiative heat and magnetic field on blood flow in an inclined tapered stenosed porous artery, *Journal of Taibah University for Science*, 14(1), 2019, 77-86.
[29] Saleem, A., Akhtar, S., Nadeem, S., Issakhov, A., Ghalambaz, M., Blood Flow Through a Catheterized Artery Having a Mild Stenosis at the Wall with a Blood Clot at the Centre, *Computer Modeling in Engineering & Sciences*, 125(2), 2020, 565-577.
[30] Hasen, S.S., Abdulhadi, A.M., Analytical Study of Soret and Dufour effect in the Electro-osmotic peristaltic flow of Rabinowitsch fluid model, *Ibn AL-Haitham Journal For Pure and Applied Sciences*, 34(2), 2021, 70-86.
[31] Akhtar, S., McCash, L.B., Nadeem, S., Saleem, S., Issakhov, A., Mechanics of non-Newtonian blood flow in an artery having multiple stenosis and electroosmotic effects, *Science Progress*, 104(3), 2021, 1–15.
[32] Saleem, A., Kiani, M.N., Nadeem, S., Akhtar, S., Ghalambaz, M., Issakhov, A., Electroosmotically driven flow of micropolar bingham viscoplastic fluid in a wavy microchannel: application of computational biology stomach anatomy, *Computer Methods in Biomechanics and Biomedical Engineering*, 24(3), 2021, 289-298.
[33] Shahzad, M.H., Awan, A.U., Akhtar, S., Nadeem, S., Entropy and stability analysis on blood flow with nanoparticles through a stenosed artery having permeable walls, *Science Progress*, 105(2), 2022, 1–34.
[34] Saleem, A., Akhtar, S., Nadeem, S., Bio-mathematical analysis of electro-osmotically modulated hemodynamic blood flow inside a symmetric and nonsymmetric stenosed artery with joule heating, *International Journal of Biomathematics*, 15(2), 2022, 2150071 .
[35] Al-Saif, A.S.J., Al-Griffi, Takia Ahmed J., A new technique to solve two-dimensional viscous fluid flow among slowly expand or contract walls, *Mathematical Modelling of Engineering Problems*, 7(4), 2020, 631-641.
[36] Al-Saif, A.S.J., Al-Griffi, T.A.J., Analytical simulation for transient natural convection in a horizontal cylindrical concentric annulus, *Journal of Applied and Computational Mechanics*, 7(2), 2021, 621-637.
[37] Ahmed, A., Nadeem, S., Shape effect of Cu-nanoparticles in unsteady flow through curved artery with catheterized stenosis, *Results in Physics*, 7, 2017, 677-689.

ORCID iD

Takia Ahmed J. Al-Griffi https://orcid.org/0000-0002-3046-7627
Abdul-Sattar J. Al-Saif https://orcid.org/0000-0002-2126-1221

How to cite this article: Al-Griffi T.A.J., Al-Saif A.S.J. Analytical Investigations for the Joint Impacts of Electro-osmotic and Some Relevant Parameters to Blood Flow in Mildly Stenosis Artery, *J. Appl. Comput. Mech.*, 9(1), 2023, 274–293.
https://doi.org/10.22055/jacm.2022.40984.3688